Phytoliths reveal Paleocene–Eocene forest expansions preceded dryland vegetation in southern South America

Elena Stiles[1,2,†], Javier N. Gelfo[3,4], Maria Sol Raigemborn[4,5], Matthew J. Kohn[6], Brielle A.D. Canares[1,2], Robin B. Trayler[7], Mauricio Ibañez-Mejía[8], Georgina Erra[4,9], Francisco Goin[3,4], and Caroline A.E. Strömberg[1,2]

[1]*Department of Biology, University of Washington, Life Sciences Building, 3747 W Stevens Way, Seattle, Washington 98195, USA*
[2]*Burke Museum of Natural History and Culture, 4303 Memorial Way NE, Seattle, Washington 98195, USA*
[3]*CONICET–División Paleontología Vertebrados, Museo de La Plata, Paseo del Bosque s/n B1900FWA, La Plata, Argentina*
[4]*Facultad de Ciencias Naturales y Museo, Universidad Nacional de La Plata, B1900 La Plata, Argentina*
[5]*CONICET–Universidad Nacional de La Plata, Centro de Investigaciones Geológicas, Diagonal 113 n. 275 1900, La Plata, Argentina*
[6]*Department of Geosciences, Boise State University, 1910 University Drive, Boise, Idaho 83725, USA*
[7]*Department of Life and Environmental Sciences, University of California, Merced, Merced, California 95343, USA*
[8]*Department of Geosciences, University of Arizona, Tucson, Arizona 85721, USA*
[9]*CONICET–División Paleobotánica, Museo de La Plata, Paseo del Bosque, s/n B1900FWA, La Plata, La Plata, Argentina*

ABSTRACT

The evolutionary history of lowland southern South American vegetation, particularly during the Paleocene–Eocene, remains enigmatic due to few existing paleobotanical records. Existing vegetation models present contradicting hypotheses ranging from expansive grasslands to tropical forests during this time. Resolving these contradictions is critical for reconstructing the ecological context surrounding the emergence of endemic South American faunas and understanding the relationship between climate and vegetation structure and composition during the warmest interval of the Cenozoic. Here, we present a basin-wide phytolith analysis from Paleocene–Eocene terrestrial deposits in the San Jorge Basin, Argentine Patagonia. These records expand existing phytolith studies and integrate new radiometric dates, providing a temporally resolved view of vegetation dynamics in the early Cenozoic. Phytolith assemblage composition suggests that forests dominated lowland ecosystems during the warm and humid Paleocene to the middle Eocene. Relative palm abundance increased between the middle and late Eocene as lowland humid megathermal forests began transitioning to progressively colder, arid, and more open vegetation, corroborated by existing paleobotanical, geochemical, and faunal records. Grasses were rare and likely represented forest understory elements until at least the early–middle Miocene, contradicting hypotheses of early Cenozoic grassy habitats in South America. Grass abundances increased between the early and middle Miocene occurred alongside the return of humid forests as temperatures and precipitation rose in the region. Sustained cooling and aridification between the middle Miocene and the Quaternary led to the rise of Patagonian steppe vegetation.

INTRODUCTION

Understanding the evolutionary history of modern biodiversity provides a foundation for exploring the processes that sustain ecosystems today and will influence them in the future (Barnosky et al., 2017). Although Neotropical and South American ecosystems have received much attention as modern biodiversity hotspots, the evolutionary origins of their floras remain enigmatic, particularly during the Paleocene–Eocene of southern South America (Wilf et al., 2013; Jaramillo, 2023). Reconstructing the vegetation history of southern South America is essential for understanding how floras responded to both local and global climate shifts and for providing direct evidence of the ecological context of faunal evolution dynamics during a key phase in early Cenozoic Patagonia (Palazzesi and Barreda, 2012; Strömberg et al., 2013). This is especially true during the Paleocene, as weakening Antarctic connections and increasing divergence between northern and southern South American biotic communities gave rise to the continent's highly endemic faunas (Palazzesi and Barreda, 2012; Jaramillo and Cárdenas, 2013; Strömberg et al., 2013; Wilf et al., 2013; Croft et al., 2020).

In the Northern Hemisphere, relatively high spatial and temporal sample resolution has allowed the characterization of regionally heterogeneous plant communities and climate during the Eocene (Utescher and Mosbrugger, 2007). In contrast, the paucity of Eocene fossil floras in South America has resulted in mainly theoretical vegetation models that provide starkly conflicting Paleogene plant biome reconstructions (Jaramillo and Cárdenas, 2013). Models of reconstructed Eocene vegetation in high South American latitudes range from tropical forests (e.g., Wolfe, 1985) or mixed forests (containing tropical, temperate, and Antarctic elements; e.g., Romero, 1986; Iglesias et al., 2011) to extensive shrublands or savannas (e.g., Ziegler et al., 2003). Available macrofloras and spore and pollen records indicate warm and humid early Eocene broadleaf forests (Wilf et al., 2005, 2013), transitioning into increasingly arid vegetation types in the middle Eocene, ultimately leading to the expansion of grasslands in the middle–late Miocene (Barreda and Palazzesi, 2007; Palazzesi and Barreda, 2007, 2012; Barreda et al., 2020). However, fossil macrofloras and pollen are poorly preserved in the Patagonian lowlands, so early Cenozoic records are temporally spotty or limited mainly to the Andean region (Barreda and Palazzesi, 2010).

In contrast to macrofloras, assemblages of microscopic plant biosilica (phytoliths) often

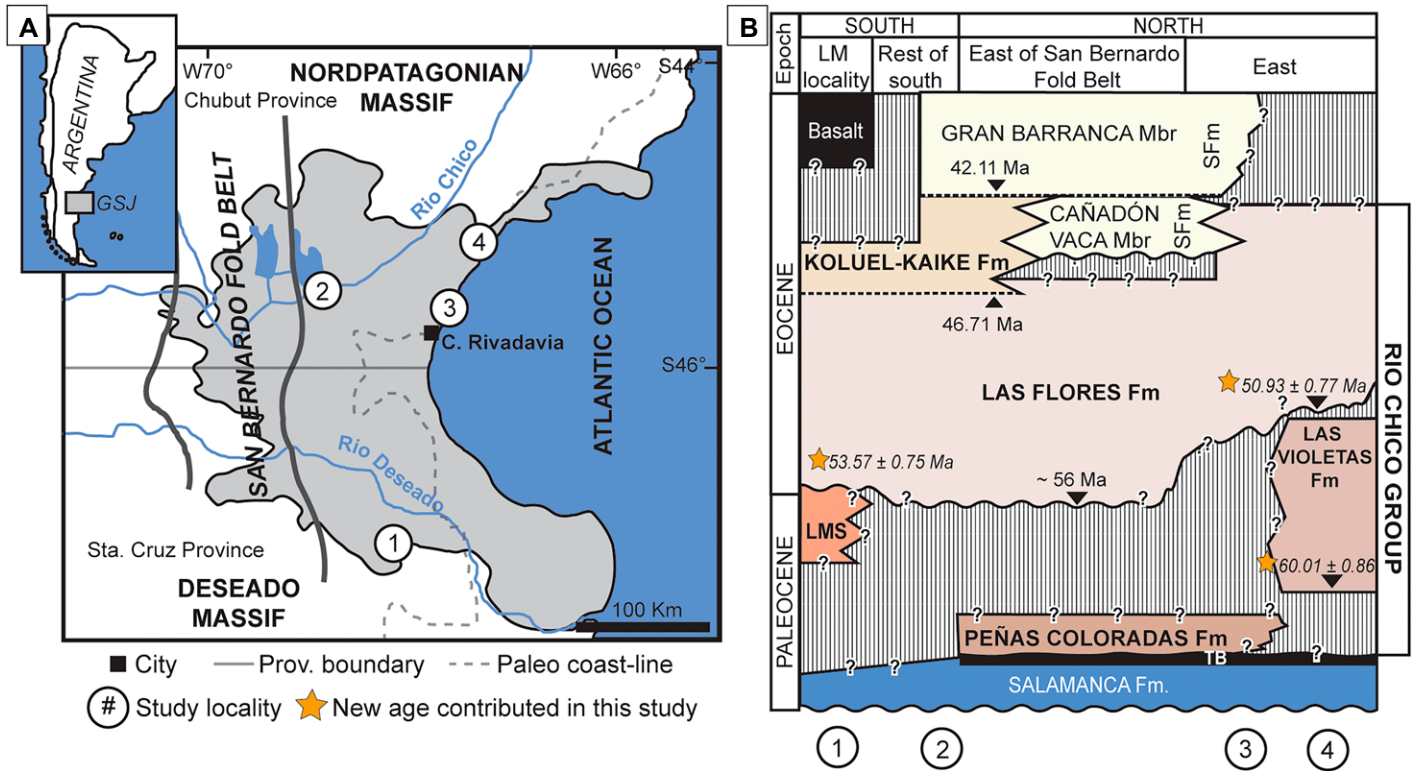Elena Stiles https://orcid.org/0000-0002-3304-7580
†elenastiles19@gmail.com

Figure 1. Geographic location of the San Jorge Basin, localities included in this study and Paleocene–Eocene stratigraphy modified after Raigemborn and Beilinson (2020) and Raigemborn et al. (2022), with updated age estimates based on new U-Pb geochronological results in this study. (A) Localities (circled numbers) within the San Jorge Basin (gray shading) in Argentine Patagonia (map modified after Raigemborn and Beilinson, 2020, and Raigemborn et al., 2022): 1—Laguna Manantiales; 2—Las Flores (this study) and Gran Barranca (Strömberg et al., 2013); 3—Rocas Coloradas; 4—Estancia Las Violetas. Approximate paleocoastline from the PALEOMAP Project Ypresian projection (Scotese and Dreher, 2012). (B) Stratigraphic chart of the studied San Jorge Basin sediments. Circled numbers correspond to localities as in panel A. Ages for the Salamanca and Transitional Beds based on Clyde et al. (2014), Rio Chico Group from Krause et al. (2017), base of Sarmiento Formation from Dunn et al. (2013), and the Laguna Manantiales (LM) and Estancia Las Violetas sections from this study. GSJ—Golfo San Jorge; LMS—Laguna Manantiales Strata; SFm—Sarmiento Formation; TB—Transitional Beds.

leave temporally continuous records, especially in well-oxidized deposits or environments not suited for preservation of other plant fossils, such as those typical of the Cenozoic of Patagonia (e.g., Barreda and Palazzesi, 2010; Zucol et al., 2010; Strömberg et al., 2013, 2018). Furthermore, phytoliths provide information relevant to reconstructing the relative abundance, composition, and ecology of grass communities and the importance of taxa often associated with tropical forests such as palms and Zingiberales (gingers), which is not readily available in macrofloras or pollen records (Piperno, 2006; Strömberg et al., 2018). Such phytolith records have provided a temporally resolved view into the middle Eocene–Miocene landscape evolution in the lowlands of Patagonia, suggesting the emergence of open aridlands by the early middle Eocene (Strömberg et al., 2013; Dunn et al., 2015; see also Zucol et al., 2018; Bellosi et al., 2021). However, comparable records have not been available for the Paleocene–early Eocene

of southern South America, preventing detailed reconstructions of the ecosystems that preceded the dry shrublands of the middle Eocene.

Here, we fill a critical gap in the record of southern South American lowland vegetation history by characterizing and interpreting new phytolith assemblages preserved in Paleocene–Eocene terrestrial deposits across the San Jorge Basin (SJB) in Argentine Patagonia (Fig. 1). Our records from multiple SJB sections significantly expand on existing phytolith studies (Brea et al., 2008; Zucol et al., 2010; Strömberg et al., 2013; Dunn et al., 2015; Zucol et al., 2018) by supplying a locally resolved, basin-wide view of vegetation change during the Paleocene–early Eocene. Herein, we contribute to ongoing work to correlate and constrain deposition in the SJB (e.g., Raigemborn et al., 2010; Dunn et al., 2013; Krause et al., 2017; Raigemborn and Beilinson, 2020; Raigemborn et al., 2022) by updating and providing new geochronologic constraints for the base of Las Violetas and Las Flores forma-

tions along the northern and southern margins of the SJB.

Within an improved temporal framework, we develop a holistic vegetation history for lowland southern South America by combining these new data with previous work on taxonomically informative micro- and macrofloras in the SJB and adjacent areas (Wilf et al., 2005; Barreda and Palazzesi, 2007; Palazzesi and Barreda, 2012; Barreda et al., 2020) and we reanalyze middle Eocene–Miocene phytolith assemblages of the SJB (Strömberg et al., 2013). Reanalysis of Strömberg et al. (2013) ensures consistent extraction and morphotype classification methods, allowing us to quantitatively analyze phytolith composition change from the Paleocene to the early–middle Miocene. This history allows us to test the early Eocene forest versus shrubland/savanna vegetation hypothesis. Our results demonstrate the likely presence of forests and other woody angiosperm-dominated or palm-dominated vegetation throughout the Paleogene

and no evidence of grassland expansion until at least the mid-Miocene.

GEOLOGICAL SETTING

The Jurassic–Miocene San Jorge Basin (SJB) is located in the southern Chubut and northern Santa Cruz Provinces of Argentine Patagonia (Fig. 1A; Fitzgerald et al., 1990; Legarreta and Uliana, 1994; Sylwan, 2001; Krause et al., 2017). Structurally, it is divided into eastern and western areas by the N-S–trending Miocene San Bernardo compressional fold belt (Sylwan, 2001, and references therein). After deposition of fluvial and volcaniclastic sediments of the Cretaceous Chubut Group, estuarine deposits of the early Paleocene (Danian) Salamanca Formation (Fig. 1B) records a regional transgression (Legarreta and Uliana, 1994; Iglesias et al., 2007; Raigemborn et al., 2010; Clyde et al., 2014; Comer et al., 2015). These Danian strata are capped by estuarine swamp deposits and paleosols of the nearly basin-wide marker beds of the Banco Negro Inferior. The Banco Negro Inferior has been interpreted as either the upper part of the Salamanca Formation (Andreis, 1977; Clyde et al., 2014; Comer et al., 2015) or part of an overlying "Transitional Beds" series (Raigemborn et al., 2010) that grade upward into the fully continental, middle Paleocene, Río Chico Group (Fig. 1A). Herein, we consider the Banco Negro Inferior as part of the "Transitional Beds" series between the marine deposition of the Salamanca Formation and the fully continental deposits of the Río Chico Group (Raigemborn et al., 2010). The "Transitional Beds" appear absent along the southeast margin of the SJB, where the Río Chico Group is instead underlain by the Salamanca Formation (Quattrocchio et al., 2024).

The early Paleocene–middle Eocene continental deposits of the northern Río Chico Group consist predominantly of high-energy fluvial deposits of the Las Violetas and Peñas Coloradas formations, transitioning upward into the increasingly lacustrine and low-energy deposits of the Las Flores and Koluel-Kaike formations (Fig. 1B; Krause et al., 2010, 2017; Raigemborn et al., 2010, 2018, 2022; Comer et al., 2015; Raigemborn and Beilinson, 2020). Along the northwestern margin of the SJB, the Las Violetas Formation is the basal unit of the Río Chico Group (Raigemborn et al., 2010). It is unconformably overlain by the Las Flores Formation, the youngest Río Chico Group unit there (Raigemborn et al., 2010; Kohn et al., 2015; Krause et al., 2017). South of the northern margin, the Las Violetas Formation is replaced by the Peñas Coloradas Formation as the basal unit of the Río Chico Group (Fig. 1B; Raigemborn et al., 2010).

Along the southern margin of the basin, the basal unit of the Río Chico Group is the newly defined Laguna Manantiales Strata, greenish siliciclastic deposits rich in plant material and palynologically distinct from the underlying Salamanca Formation (Quattrocchio et al., 2024). The Laguna Manantiales Strata underlie the Las Flores Formation, which is in turn overlaid by the volcanoclastic Koluel-Kaike Formation as the youngest formation of the Río Chico Group (Fig. 1A; Raigemborn et al., 2010; Krause et al., 2017). The Las Flores and Koluel-Kaike formations along the western and southern SJB are overlain by the middle-late Eocene, pedogenically modified fluvial and aeolian deposits of the lower Sarmiento Formation (Raigemborn et al., 2010; Dunn et al., 2013; Raigemborn and Beilinson, 2020).

The Sarmiento Formation contains mostly volcanic material reworked through fluvial and aeolian transport, later modified by pedogenic processes (Spalletti and Mazzoni, 1979). In the area of Las Flores/Gran Barranca (Fig. 1A), the Sarmiento Formation is subdivided into (in stratigraphic order) the Gran Barranca, El Nuevo, Rosado, Puesto Almendra Inferior, Vera, Puesto Almendra Superior, and Colhue Huapi members, deposited between 42.11 Ma and 18.5 Ma (Ré et al., 2010; Dunn et al., 2013). North of the Las Flores/Gran Barranca localities, the Gran Barranca Member is underlaid by the Vaca Member (e.g., Krause et al., 2017) in sites not analyzed in this study.

Correlating depositional units in the Paleogene SJB has been historically challenging, yet it is essential for reconstructing broad evolutionary patterns in South American floras and faunas (e.g., Clyde et al., 2014; Krause et al., 2017). Efforts to temporally constrain early Paleogene deposition in the SJB have included sedimentological, magnetostratigraphic, and geochronological approaches (e.g., Raigemborn et al., 2010; Dunn et al., 2013; Clyde et al., 2014; Comer et al., 2015; Krause et al., 2017; Raigemborn et al., 2022; Fig. 1B).

METHODS

Sedimentary rock samples from the Banco Negro Inferior, Transitional Beds, and Río Chico Group units (Las Violetas, Peñas Coloradas, Las Flores, and Koluel-Kaike formations) were collected, from north to south, in the Estancia Las Violetas, Bajo Palangana (in the general area of Rocas Coloradas following Raigemborn et al., 2010), Las Flores, and Laguna Manantiales localities (Figs. 1 and 2; Raigemborn et al., 2010, 2022). These samples were obtained during 2009–2018 field campaigns for phytolith and geochronological analyses.

Geochronology

Tuffaceous sandstones were collected for U-Pb detrital zircon estimations from the Las Flores Formation at the Laguna Manantiales and Estancia Las Violetas localities, as well as from the base of the Las Violetas Formation at Estancia Las Violetas (Fig. 2). Analyses were conducted using laser ablation–inductively coupled plasma–mass spectrometry (LA-ICP-MS) at Boise State University, Boise, Idaho, USA, and at the Arizona LaserChron Center, University of Arizona, Tucson, Arizona, USA, for Estancia Las Violetas and Laguna Manantiales samples, respectively.

Estancia Las Violetas

Methods for zircon analysis followed standard protocols at Boise State University (Macdonald et al., 2018; Trayler et al., 2020). Broadly, analysis required separation of zircon, mounting select sharply faceted grains in epoxy, polishing to zircon interiors, imaging using cathodoluminescence, LA-ICP-MS analysis for U-Th-Pb isotopes and trace element compositions, data reduction using in-house software, and determination of weighted mean dates for the youngest age populations using IsoplotR (Vermeesch, 2018). Age uncertainties combine both spot-specific counting statistics (which vary) and calibration uncertainties of ~1.2‰. The data file in the Supplemental Material[1] contains analytical and standardization details.

Laguna Manantiales

U-Pb detrital zircon ages for the base of the Laguna Manantiales section were determined using LA-ICP-MS using a NU Plasma multicollector ICP-MS and Teledyne Photon Machines Analyte G2 ArF excimer (193 nm) laser ablation system at Arizona LaserChron Center. Instrumental bias, drift, and inter-element fractionation corrections were performed by standard-sample bracketing, using FC-1 zircon with a well-established chemical abrasion–isotope dilution–thermal ionization mass spectrometry (CA-ID-TIMS) $^{206}Pb/^{238}U$ age of 1095.97 ± 0.68 Ma (Ibañez-Mejia and Tissot, 2019) as primary reference material. U-Pb analyses were performed using a laser-beam diameter of 30 µm and simultaneously measuring ^{238}U, ^{232}Th, ^{208}Pb, ^{207}Pb, and ^{206}Pb in Faraday cups, while $^{204}(Pb + Hg)$ and ^{202}Hg were measured

---
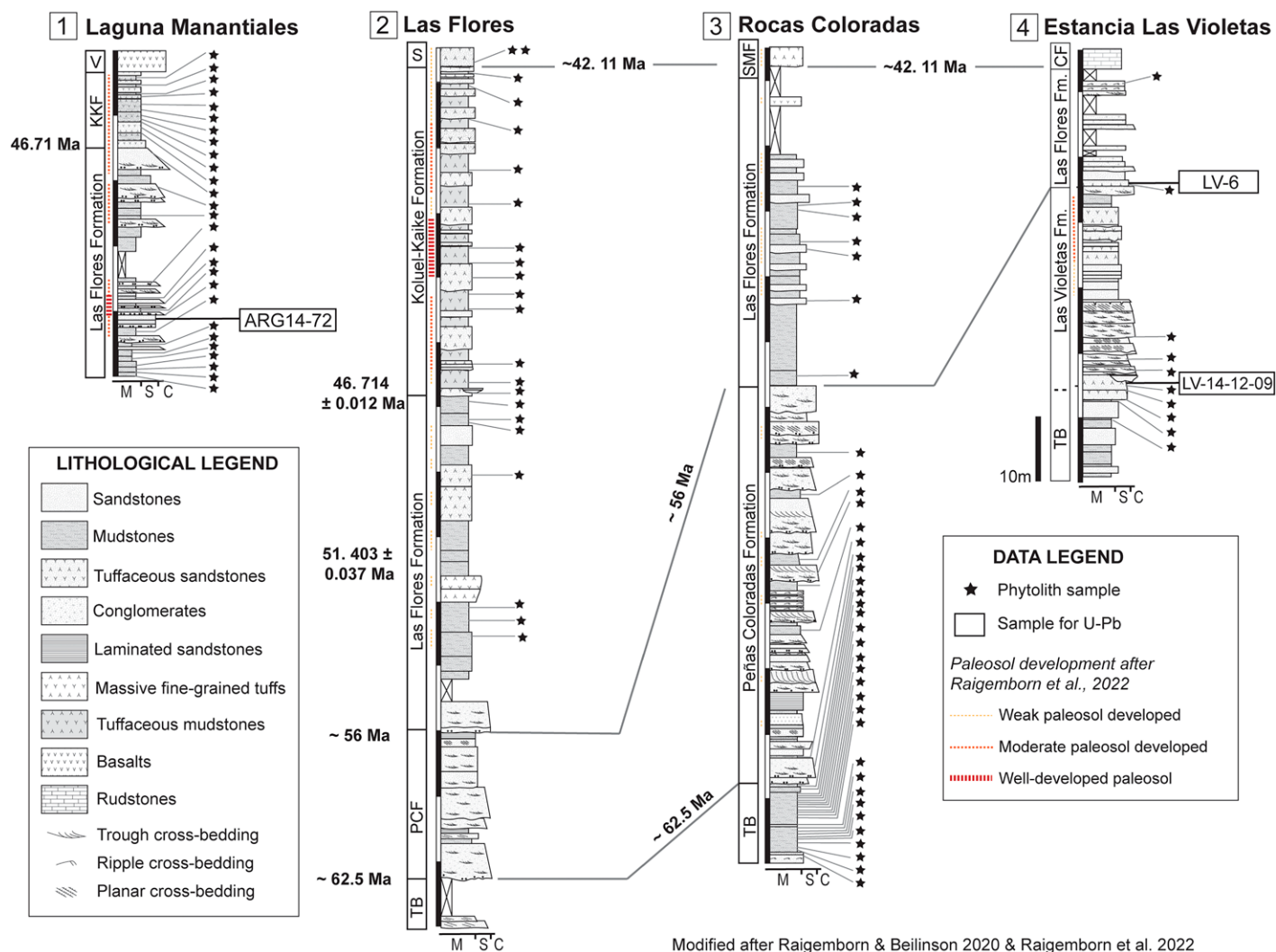
Figure 2. Distribution of phytolith and geochronology samples across our studied localities. 1—Laguna Manantiales; 2—Las Flores; 3—Rocas Coloradas; 4—Las Violetas. Modified after Raigemborn and Beilinson (2020), with age constraints compiled from Dunn et al. (2013), Clyde et al. (2014), and Krause et al. (2017). See the Supplemental Material for reference numbers and sample-specific results (see text footnote 1). CF—Chenque Formation; KKF—Koluel-Kaike Formation; PCF—Peñas Coloradas Formation; S & SMF—Sarmiento Formation; TB—Transitional Beds; V—volcanics; M, C, S—mudstones, conglomerate, sandstone.

using discrete-dynode secondary ion multipliers. Data collection and processing follow the methods of Sundell et al. (2021). Zircon crystals from Fish Canyon Tuff (ca. 28.5–28.2 Ma; Wotzlaw et al., 2013), R33 (419.26 ± 0.38 Ma; Black et al., 2004), and SL-F (555.86 ± 0.68 Ma; Wang et al., 2023) were analyzed as secondary reference materials and treated as unknowns, to evaluate session accuracy. Calculated mean ages for these secondary reference materials are 28.08 ± 0.43 Ma (2σ, n = 5, mean square of weighted deviates [MSWD] = 2.3) for Fish Canyon, 421.9 ± 4.8 Ma (2σ, n = 5, MSWD = 0.21) for R33, and 556.0 ± 5.3 Ma (2σ, n = 15, MSWD = 0.16), which are within uncertainty of their respective reference values.

Age Model

To place new samples in a temporal framework, we generated age-depth models for each stratigraphic section using ModifiedBChron, a Bayesian age-depth model modified to allow the use of deep-time geochronologic data, including $^{40}Ar/^{39}Ar$ and U-Pb (Haslett and Parnell, 2008; Trayler et al., 2020). In our implementation, prior distributions were assigned based on the type and associated uncertainty of each age constraint: absolute dates were modeled using normally distributed priors, while magnetostratigraphic constraints were assigned uniformly distributed priors with uncertainties equal to half the duration of the chron (see the Supple-

mental Material for section-specific constraints and results). The model interpolates between the known age constraints to estimate ages continuously along each section. We combined previously published age constraints for each section (Dunn et al., 2013; Clyde et al., 2014; Krause et al., 2017) with the new ages presented here. The existing age model from Strömberg et al. (2013) was used for the Sarmiento Formation.

Phytolith Analysis

Sedimentary rock samples were processed for phytoliths using modified standard methods, comprising chemical and mechanical steps to isolate biosilica particles (see Strömberg et al.,

2013, 2018). Approximately 1 g of sediment per sample was homogenized using a mortar and pestle, after which carbonates and organic matter were removed using hydrochloric acid and Schultze's solution, respectively. Particles >250 μm in diameter were removed via sieving. Clays were removed via repeated washing, sieving, centrifuging, and decanting, and biosilica particles were isolated from the remaining sediment by heavy liquid (a zinc bromide solution with specific gravity 2.38) flotation. Extracted biosilica samples are housed in the Burke Museum of Natural History and Culture, University of Washington, Seattle, Washington, USA (UWBM); duplicate slides are reposited in the Argentinian Museo Regional Provincial Padre Jesus Molina (Rio Gallegos, Santa Cruz Province) and Universidad Nacional de La Patagonia San Juan Bosco (Comodoro Rivadavia, Chubut Province; Tables S2 and S3). Extracted particles were fixed on microscopy slides using Meltmount, scanned, and counted at 1000× magnification under a compound microscope. The abundance and preservation of phytoliths within each sample were assessed following Strömberg et al. (2018; Table S1). Poorly preserved samples with significant breakage, internal structure alteration, or dissolution of phytoliths were excluded from analysis but were described qualitatively (Fig. S4).

At least 200 diagnostic phytoliths per sample were tallied (Strömberg, 2009). Phytolith morphotype classification followed Strömberg (2003) and Strömberg et al. (2013), grouping morphotypes into broad plant functional groups. Major plant functional groups relevant to this study include the following. (1) Conifers, Woody and Herbaceous Dicotyledonous angiosperms, Fern, Cycad, and Ginkgo. These groups are collectively referred to as forest indicators (FI) based on their broad ecological preferences (Strömberg et al., 2018). (2) Grasses (Poaceae family) of open and closed habitats (represented by grass silica short cell phytoliths [GSSCPs]). (3) Palms. (4) Zingiberales (ginger relatives) and (5) Aquatic Plants. Classifications are based on the UWBM phytolith reference collection and phytolith reference literature (e.g., Strömberg, 2003; Piperno, 2006). Morphotypes not defined in Strömberg (2003) were described following the International Code for Phytolith Nomenclature (ICPN) 2.0 (Neumann et al., 2019; see the Supplemental Material). Non-diagnostic morphotypes are also identified but not used for interpretation. These morphotypes either appear in a broad range of taxa or their production is not proportional to the contributed biomass (Strömberg et al., 2018).

In addition to the plant functional groups, we analyzed changes within trees and shrubs, excluding palms within the FI group. We compared our results with those of Strömberg et al. (2013), given that they were obtained using the same extraction, counting, and morphotyping methods. To ensure a consistent comparison, accounting for potential variability in morphotype assignment between investigators, we took a conservative approach, simplifying morphotype counts by using broader categories encompassing similar shapes (e.g., spherical and subspherical bodies; Table S5). Although these groups do not correspond directly to specific taxa, their abundance variation in phytolith assemblages should signal shifts in plant community composition (e.g., Zucol et al., 2010). We applied the subsequent analyses to the simplified morphotype count matrices (Table S11).

The relative abundances of plant functional groups within diagnostic counts were calculated, and 95% confidence intervals were estimated using bootstrapping (n = 10,000; Strömberg, 2009). In each studied locality, we applied locally estimated scatterplot smoothing (Cleveland and Devlin, 1988) to test for temporal trends in mean abundances of major plant functional groups (see the Supplemental Material for method description and considerations). Principal components analysis and hierarchical cluster analysis were used to investigate possible composition-driven groupings within major functional groups across space and time. We excluded morphotypes counted <10 times across all studied samples and normalized the resulting matrix using a logarithmic transformation to reduce the effect of count variability. Samples and associated compound variables (formation, age, study site) were clustered using a pairwise Euclidean distance matrix and linked through Ward's method. In addition, we tested for temporal variation in canopy structure using reconstructed Leaf Area Index, a method based on epidermal phytolith morphology (Dunn et al., 2015). All analyses were conducted in R v.4.4.0 (see the Supplemental Material).

RESULTS

New U-Pb Ages

Estancia Las Violetas

Twenty-five spot analyses for sample LV-14-12-09 include two inherited Mesozoic grains, then a temporally coherent distribution with apparent ages of ca. 60 Ma (Fig. 3A). Omitting one young statistical outlier, 22 analyses define an age of 60.01 ± 0.58 Ma (internal 2σ errors only; total error is ± 0.86 Ma, 2σ), with a probability of fit of 0.072. Fifty spot analyses for sample LV-6 include three inherited grains with Paleozoic and Mesozoic ages, then a broad

distribution with apparent ages ranging from ca. 60 Ma to ca. 50 Ma (Fig. 3B). The youngest, statistically coherent population of ages includes 34 grains with an average age of 50.93 ± 0.40 Ma (internal 2σ errors only; total error is ± 0.77 Ma, 2σ), with a probability of fit of 0.074. We interpret the ages of 60.01 ± 0.86 Ma and 50.93 ± 0.77 Ma to represent the timing of deposition for these strata.

Laguna Manantiales

The volcaniclastic horizon from the base of the Laguna Manantiales section yielded a complex age spectrum, with individual zircon dates ranging from ca. 1050 Ma to 53 Ma (Fig. 3C), consistent with sedimentary reworking. To obtain the most likely maximum depositional age for this horizon, 300 zircon crystals were analyzed. Thirteen of the analyzed zircons yielded Cenozoic ages, and the youngest five grains define a coherent cluster with a weighted mean $^{206}Pb/^{238}U$ age of 53.57 ± 0.59 Ma (2σ; analytical uncertainty only). Including propagation of within-session random and systematic uncertainties yields a final $^{206}Pb/^{238}U$ age of 53.57 ± 0.75 Ma (2σ, n = 5, MSWD = 0.89), which includes analytical uncertainty, uncertainty on the ID-TIMS date of the primary reference material, normalization uncertainty for sample-standard bracketing, non-radiogenic Pb correction of uncertainty, and ^{238}U decay constant uncertainty.

Phytolith Preservation and Assemblages

Phytolith preservation and recovery are uneven across the sampled localities and appear to be positively correlated with ash and silt content of the sediment (see the Supplemental Material). Claystones and fine to coarse-grained sandstones produced the least consistent recovery and worst preserved phytoliths, in line with published observations (e.g., Zucol et al., 2010; Strömberg et al., 2018). Paleosol development (Raigemborn et al., 2018, 2022; Raigemborn and Beilinson, 2020) does not correlate with preservation quality, but beds with carbonaceous material, such as the Transitional Beds (Raigemborn et al., 2010), yielded most of the poorly preserved samples. Non-phytolith biosilica (freshwater sponge spicules and occasional diatom fragments) are sparse to moderately abundant in individual samples and occur in 53% and 69% of the samples, respectively. They appear in fine-grained beds interbedded with coarser-grained and often cross-bedded channel deposits. Chrysophyte cysts are present in ∼24% of samples but are rare overall.

Phytolith assemblages are overwhelmingly dominated by Palm and FI morphotypes. In general, palm-associated morphotypes inversely
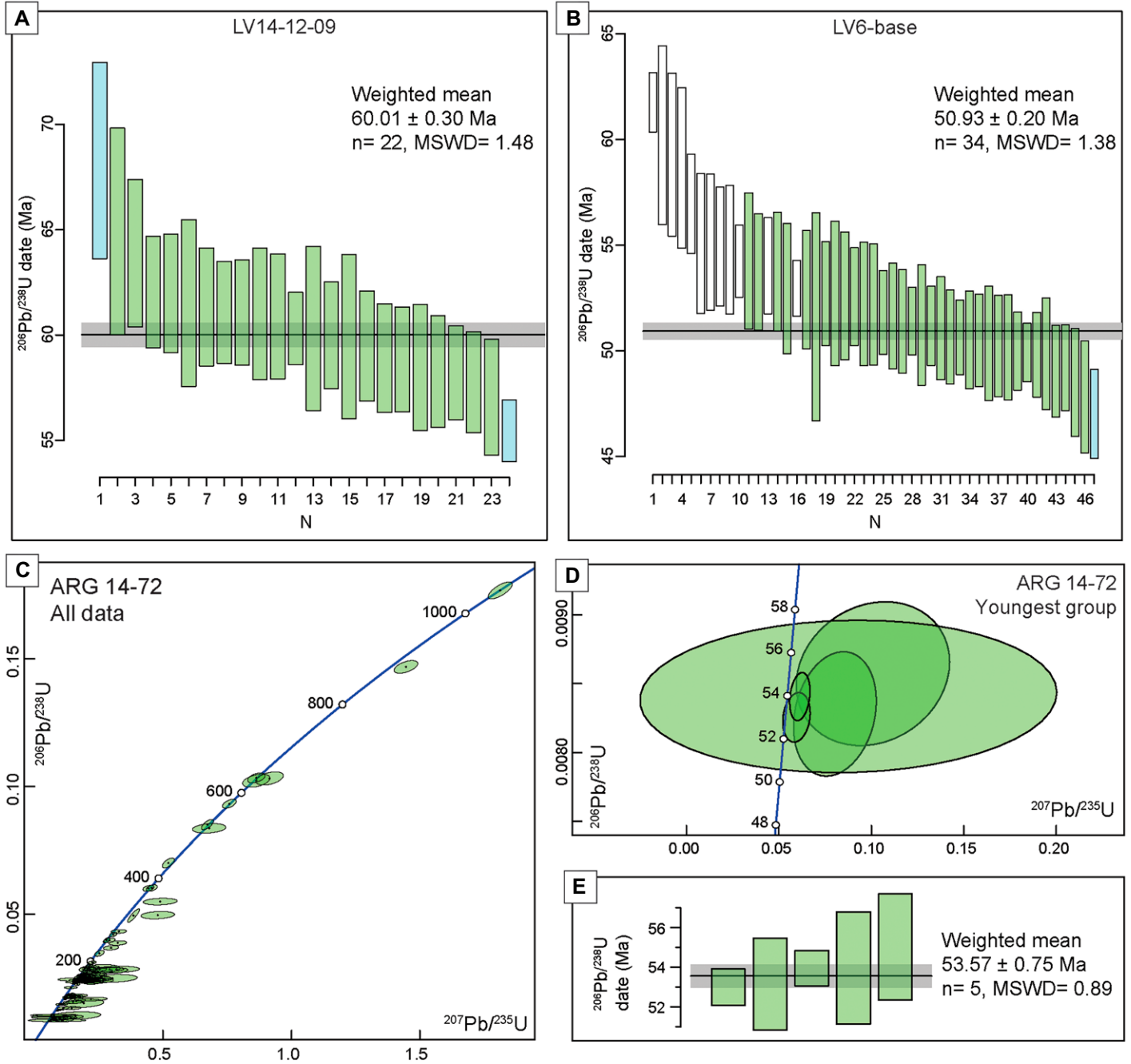
Figure 3. Zircon U-Pb geochronology for Estancia Las Violetas (A, B) and Laguna Manantiales (C–E). (A) Ranked age plot of laser ablation–inductively coupled plasma–mass spectrometry (LA-ICP-MS) U-Pb dates from sample LV-14-12-09. Green bars are included in the weighted mean age; blue bars are statistical outliers and were not included in the mean age. (B) Ranked age plot of LA-ICP-MS U-Pb dates from sample LV6-base. Green bars are included in weighted mean age; white bars were manually removed from weighted mean age; blue bar is a statistical outlier and was not included in the mean age. (C, D) U-Pb concordia diagrams from chemical abrasion–isotope dilution–thermal ionization mass spectrometry (CA-ID-TIMS) analytical results for the tuffs analyzed in sample ARG14-72. (E) Ranked age plot of LA-ICP-MS U-Pb dates from sample ARG14-72. Green bars are included in the weighted mean age. MSWD—mean square of weighted deviates.

correlate with non-diagnostic forms, indicating that non-diagnostic forms were primarily produced by FI taxa. Palm-derived Spheroid echinate (morphotype Clm-2 in Strömberg, 2003;

Fig. 4A) is the single most common morphotype observed in all our samples, representing up to 56% of the total count in palm-dominated assemblages. Aquatic Plants and Zingiberales

are rare, representing <2% in four and one sample, respectively. GSSCPs constitute <1% of total counts in five samples, with a maximum of only ~7% in two samples in the Las Flores
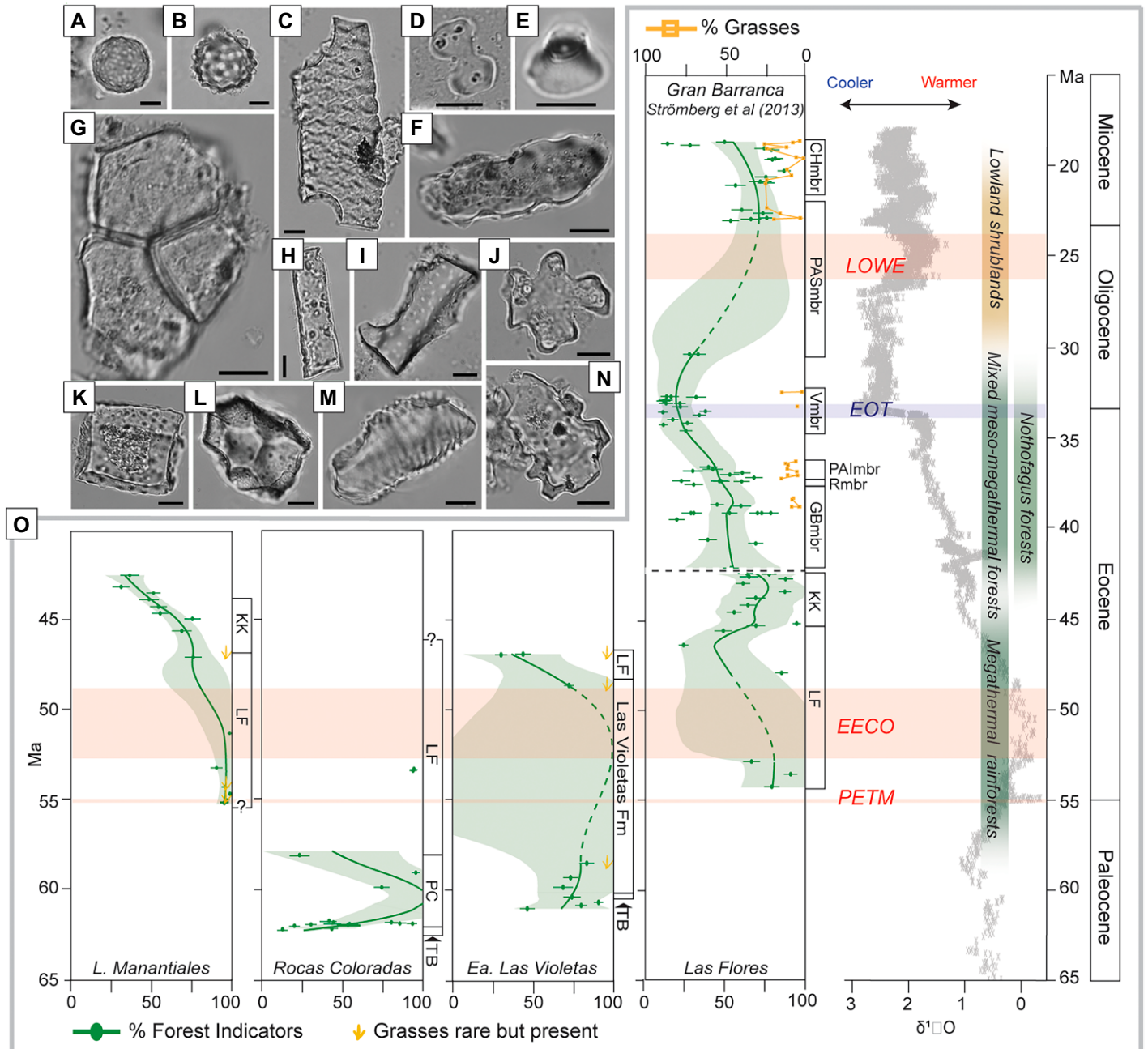
Figure 4. (A–N) Selected phytolith morphotypes in phytolith assemblages of the Paleocene–Eocene San Jorge Basin. International Code for Phytolith Nomenclature (ICPN) 2.0 (Neumann et al., 2019) name (when applicable) in parenthesis. (A) Cl⁻³. (B) Clm-2 (SPHEROID ECHI-NATE). (C) Tra-F2, vessel element phytolith. (D) Bi-7 (BILOBATE) grass silica short cell phytolith (GSSCP). (E) CO-1A (RONDEL) GSSCP. (F) CE-1 (CRENATE) GSSCP. (G) Epi-1 polygonal epidermal phytolith. (H) Elo-1 (ELONGATE ENTIRE) epidermal phytolith. (I) Scl-7A, sclereid phytolith. (J) Epi-2, anticlinal epidermal phytolith. (K) Blo-F2, blocky phytolith. (L) Blo-11 blocky phytolith. (M) Tra-2 (TRACHEARY ANNULATE). (N) SclF-1, sclereid phytolith. Phytoliths A, C, G, and I–N are forest indicators; H is a common but non-diagnostic phytolith; B is a palm indicator; D–F are GSSCPs (see text), associated with open-habitat grasses. Scale bar = 10 microns. (O) Temporal trends in the relative abundance of forest indicators within diagnostic counts, combining the results from this study and Strömberg et al. (2013). Ages of stratigraphic units in the Sarmiento Formation from Dunn et al. (2013); samples of Laguna Manantiales, Rocas Coloradas, Estancia Las Violetas, and Las Flores localities placed in a temporal framework using ModifiedBChron (see text for details; Trayler et al., 2020). Global δ¹⁸O curve and warming events from Zachos et al. (2001). KK—Koluel-Kaike Formation; LF—Las Flores Formation; PC—Peñas Colo-radas Formation; TB—Transitional Beds; mbr suffix—member of the Sarmiento Formation; GBmbr—Gran Barranca; Rmbr—Rosado; PAImbr—Puesto Almendra Inferior; Vmbr—Vera; PASmbr—Puesto Almendra Superior; CHmbr—Colhue Huapi; PETM—Paleocene Eocene Thermal Maximum; EECO—Early Eocene Climatic Optimum; EOT—Eocene Oligocene Transition; LOWE—Late Oligocene Warming Event. Eocene–Miocene Patagonian vegetation trends from Barreda and Palazzesi (2007).
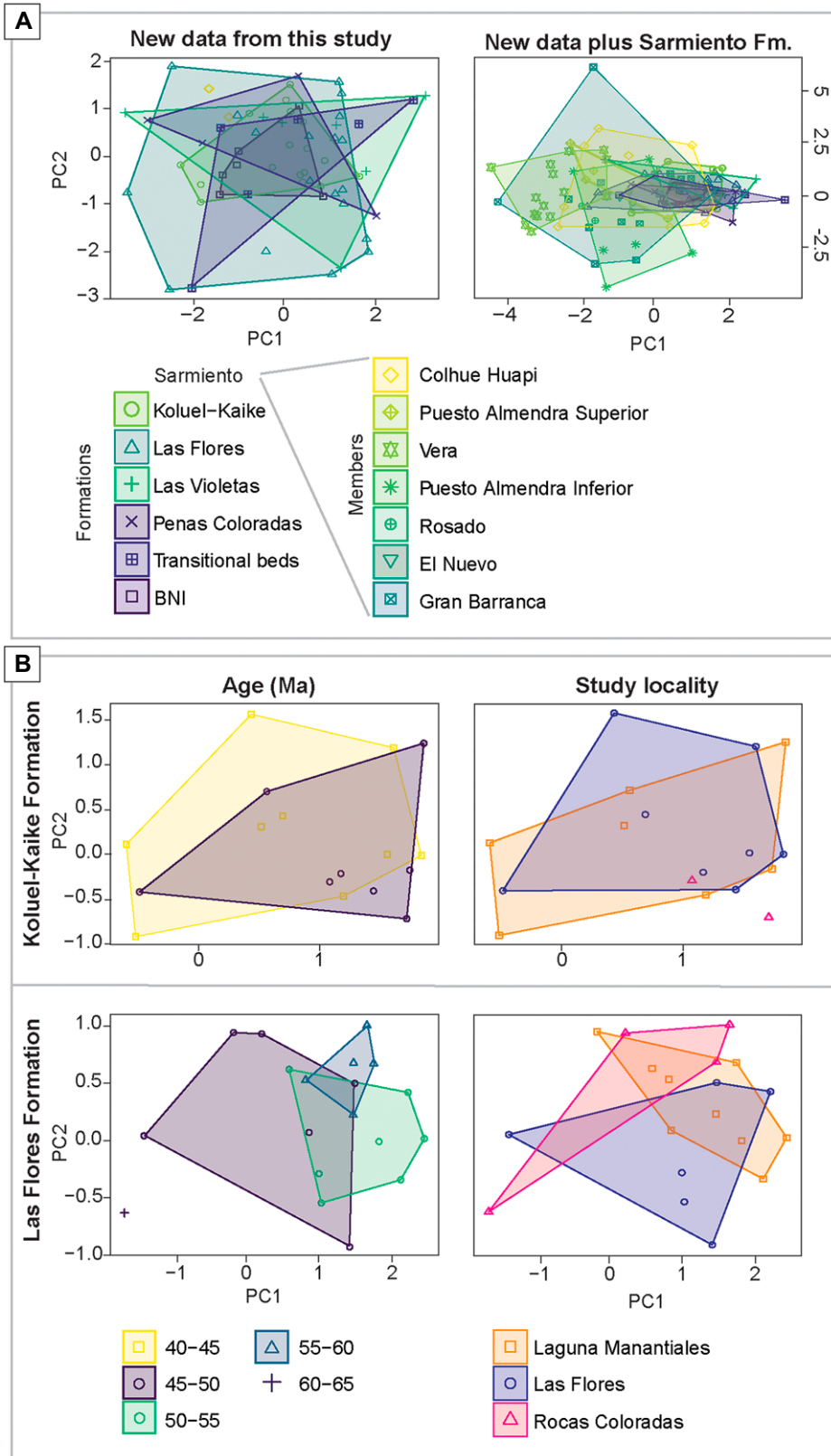
Figure 5. The composition of forest indicator phytoliths through time and space in the San Jorge Basin, as visualized through principal component analysis (PCA). (A) PCA of new Paleocene–Eocene assemblages only (left) and new data plus the seven members of the Sarmiento Formation (right). (B) Comparison of spatial and temporal patterns across the Koluel-Kaike (top row) and Las Flores (bottom row) formations. Left panel for each represents PCA of individual samples grouped by 5 Ma time bin, while right panel shows PCA groupings by study locality.

coideae, Aristidoideae, Chloridoideae, Micrairoideae, Arundinoideae, and Danthonioideae; Soreng et al., 2022), or conical rondels (Fig. 4E) often associated with the BOP clade (Bambusoideae, Oryzoideae, and Pooideae; Soreng et al., 2022; Fig. 4). GSSCP morphotypes in Laguna Manantiales are strongly associated with grasses within the BOP clade (e.g., Strömberg et al., 2013; Peppe et al., 2023), specifically the Pooideae.

Principal Components Analysis Results

Principal components analysis shows that the overall compositions of FI morphotype assemblages strongly overlap across formations within the Río Chico Group. However, the degree of compositional heterogeneity varies through depositional environment, space, and time (Fig. 5A). Assemblages from estuarine swamp deposits and paleosols of the Banco Negro Inferior marker bed are the most homogeneous, followed by the rest of the Transitional Beds. All units of Río Chico Group overlap significantly, with assemblages from the Las Flores Formation being the most heterogeneous (Fig. 5A). Fluvial deposits of the Las Flores and Koluel-Kaike formations are the most widely distributed across our study area and show significant overlap both in terms of FI composition across localities and across 5 Ma time bins (Fig. 5B). Nonetheless, there is more overlap across studied localities than age bins, independently of the overall percentage of FI in the samples (Fig. 5B).

The overlying Sarmiento Formation FIs are significantly more heterogeneous and show more internal temporal variability than the underlying formations combined (Fig. 5A). The basal Gran Barranca member is most compositionally diverse. All members of the Sarmiento Formation except the Vera Member overlap with the Río Chico Group (Fig. 5A). The Vera Member spans the Eocene–Oligocene

Formation in Laguna Manantiales; non-diagnostic grass phytoliths (e.g., epidermal phytoliths) are also rare (Table S7). In samples where GSS-CPs represent <1% of counts, morphotypes are either bilobates (Fig. 4D) typical of members of the PACMAD clade (Poaceae subfamilies Pani-

Transition (EOT) and forms the most distinct and internally homogeneous unit (Fig. 5A). Palms overwhelmingly dominate the Vera Member, while higher proportions of both FI and grasses characterize both the stratigraphically lower and higher Puesto Almendra Inferior and Puesto Almendra Superior. The Puesto Almendra Superior first shows a transition to moderately abundant grass communities (up to 25% of diagnostic morphotypes; Strömberg et al., 2013), dominated by pooid open habitat grasses in the early Miocene.

Cluster Analysis

The hierarchical cluster analysis on FI composition across all samples shows that time interval, rather than locality, primarily dictates clustering (Fig. 6). Sample-based (Q-mode) hierarchical cluster analysis identifies three main clusters based on the dominant 5 Ma age bins of the samples. Grouped by epoch, these are Paleocene–early Eocene (i.e., Transitional Beds, Peñas Coloradas, Las Violetas, and the base of Las Flores formations), middle–late Eocene (Las Flores, Koluel-Kaike, and Sarmiento formations), and Eocene–Oligocene transition (Sarmiento Formation; Fig. 6A). Variable-based (R-Mode) hierarchical cluster analysis of relationships among 5 Ma age groups further supports this pattern, forming distinct Paleocene–early Eocene, and Eocene–Oligocene transition clusters (Fig. 6B). Notably, samples from the EOT and adjacent time bins form a strikingly homogeneous cluster in both Q- and R-modes (Fig. 6). In contrast, the remaining two clusters in Q-mode analysis are more heterogeneous. R-mode analysis shows that middle Eocene assemblages are most like those of the early–middle Miocene, followed by Paleocene–early Eocene assemblages (Fig. 6B).

Compositionally, palm phytoliths dominate the EOT and adjacent assemblages (40–30 Ma) of the Puesto Almendra Inferior and Superior members (Figs. 6A and 6B), while FIs dominate the remaining clusters. FI composition also appears to be largely driven by time rather than space. For example, FI assemblages in Las Flores and Laguna Manantiales, which are separated by >200 km, both capture the early to middle Eocene Las Flores and Koluel-Kaike formations. The overall FI composition of these localities is more similar to each other than to localities that are geographically closer (Fig. 6C).

Reconstructed Leaf Area Index

Reconstructed Leaf Area Index values for 13 samples distributed across the Laguna Manantiales, Rocas Coloradas, and Estancia Las Violetas sites show no discernible trend across space and time. Values ranged from 0.44 to 2.07, corresponding to desert/shrublands and wet deciduous forests, respectively. Our interpretations did not include these results (see the Supplemental Material for discussion).

DISCUSSION

Improved Geochronological Framework

Our results refine the only existing age constraint for the base of the Las Violetas Formation and provide new geochronological data for the Las Flores Formation at both the northern (i.e., the Estancia Las Violetas locality) and southern (i.e., the Laguna Manantiales locality) margins of the San Jorge Basin (SJB). In the Cañadón Hondo locality (~50 km west of the Estancia Las Violetas), Andreis (1977) produced a radiometric age of 61 ± 5 Ma for the transitional levels (then considered the top of the Salamanca Formation) separating the Salamanca and Las Violetas formations. To date, this had been the only constraint on the age of the Las Violetas Formation. Our new date places the base of Las Violetas Formation at 60.01 ± 0.58 Ma, providing significantly lower uncertainty, and a better-constrained age model for the sequence outcropping at the Estancia Las Violetas locality. Basin-wide, the base of the Las Flores Formation has been inferred to be at least ca. 56 Ma, based on an erosional unconformity with the underlying Las Violetas and Peñas Coloradas formations linked to a global sea-level fall (Krause et al., 2017). This interpretation is consistent with our age estimate for the lower Las Flores Formation along the southern SJB (Laguna Manantiales; 53.57 ± 0.59 Ma); however, our results from the northern margin (i.e., Estancia Las Violetas) place the base of the Las Flores Formation at 50.93 ± 0.40 Ma. This result, coupled with differences in thickness, sedimentary facies, and paleosol types of this unit across various locations in the SJB, could suggest diachronous deposition of the Las Flores Formation between the northern and southern SJB, or that the base of the Las Flores Formation is not preserved along the northern margin of the basin. Without additional age constraints for the top of Las Violetas or Peñas Coloradas formations, it is not possible to rule out either possibility.

Our new geochronological results provide the first two absolute age constraints the base of the Las Flores Formation, as well as the first revised age estimate for the base of Las Violetas Formation in Estancia Las Violetas (Fig. 1B). The base of the Las Flores Formation at both Estancia Las Violetas and Laguna Manantiales localities
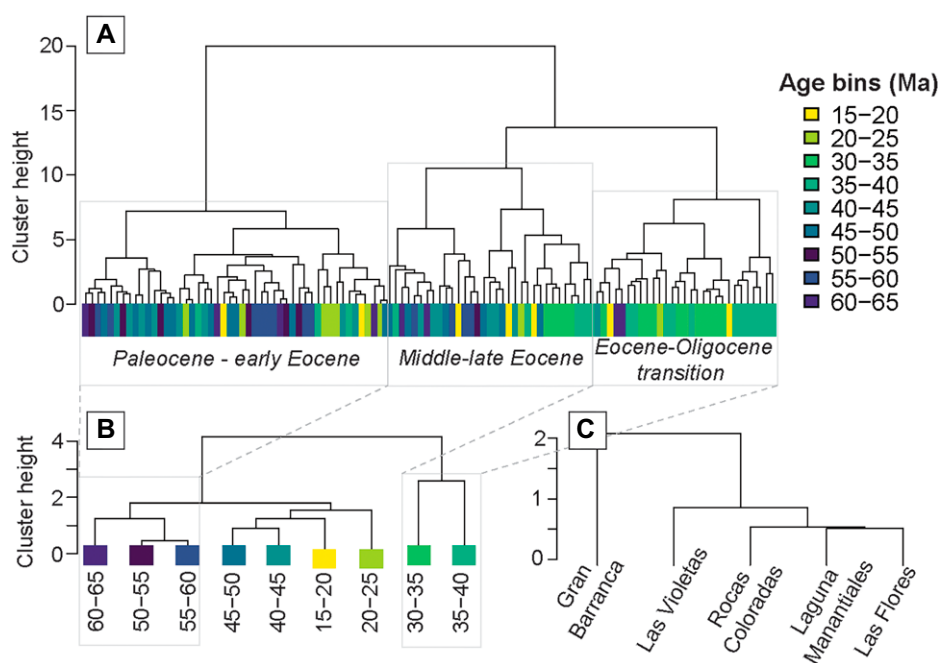

Figure 6. The composition of forest indicator phytoliths through time and space in the San Jorge Basin, as visualized through a two-way hierarchical cluster analysis (HCA). (A) Sample HCA, highlighting three clusters characterized by the most common 5 Ma age bins and their geological ages. (B) Age bins clustered by composition. (C) Localities clustered by composition.

appears to be younger than previously inferred (ca. 56 Ma), suggesting that sedimentation was delayed due to global sea-level fall, it remains unclear if it was diachronous across the SJB. Further work is needed to clarify this. The age of the lower Las Flores Formation in Laguna Manantiales indicates that the Early Eocene Climatic Optimum (EECO) is captured at least in this section, in agreement with interpretations based on the paleosol type and the degree of paleosol development (i.e., Ultisol- and Plinthitic Ultisol–like paleosols; Raigemborn et al., 2022). The base of the Las Violetas Formation is older than previously estimated, shifting from the late to the middle Paleocene. Although it is unclear whether the EECO could be preserved in Estancia Las Violetas given the erosional unconformity at the base of the Las Flores Formation, it is possible that it is preserved near the upper exposure of the Las Violetas Formation, where strongly developed paleosols (i.e., Alfisol-like paleosols) are present (Raigemborn et al., 2022).

No Early Cenozoic Grasslands in Southern South America

The scarcity of grass phytoliths in our biosilica assemblages stands against models suggesting early Eocene savannas in southern South America (e.g., Ziegler et al., 2003). Instead, our results align with previous interpretations of grasses as rare understory components in Paleocene–middle to late Eocene assemblages (e.g., Raigemborn et al., 2009). Some previous studies in the SJB proposed the rise of (sub) tropical C_4 grasslands in Argentine Patagonia by 40 Ma based on PACMAD-associated GSSCPs in middle Eocene phytolith assemblages of the Koluel-Kaike and Sarmiento formations (Zucol et al., 2010, 2018; Bellosi et al., 2021) as well as sedimentology, paleopedology, and the fossil record of dung beetle brood balls (Sánchez et al., 2010; Bellosi and Krause, 2014; Bellosi et al., 2021). If this scenario were accurate, we would expect to find PACMAD-associated morphotypes in high abundances ($\sim$>35% and typically >50%) in our middle Eocene phytolith assemblages (e.g., Strömberg et al., 2013; Peppe et al., 2023). In contrast, only a small subset of our Paleocene to middle Eocene assemblages contains identifiable grasses, and even when present, GSSCPs constitute a small fraction of diagnostic morphotypes (<10%). These results are consistent with other methodologically similar phytolith studies in the Sarmiento Formation (e.g., Strömberg et al., 2013; Dunn et al., 2015), as well as palynological and macrofossil studies from Patagonia (Barreda and Palazzesi, 2007; Palazzesi and

Barreda, 2012). Grasses were rare until the middle-late Eocene (Fig. 5B) and were unlikely to have been dominant components of the landscape during this time.

Several factors may explain the discrepancy between our findings and earlier phytolith-based reconstructions that suggest the Eocene emergence of grasslands. First, the phytolith extraction protocol and morphotype counting in earlier studies differ from those applied in this study. Previous analyses separated phytoliths by size fraction (5–53 µm and 53–250 µm), counted each fraction independently, and later combined datasets to make interpretations (Zucol et al., 2010, 2018; Bellosi et al., 2021). This method, paired with extractions from individual plant species, is commonly applied in Quaternary phytolith studies to identify plant groups that may be over- or underrepresented in the assemblage (Piperno, 2006; Iriarte and Paz, 2009; Dickau et al., 2013; Piperno and McMichael, 2020). While this method is effective for modern calibration studies, we argue against applying it to fossil assemblages as it may skew the interpretation of assemblage composition by overrepresenting phytoliths within either size class (by ignoring the relative abundance of size fractions in the assemblages overall) while providing little insight into the taxonomic composition of the flora from which it originates (Strömberg et al., 2018; Crifò and Strömberg, 2021).

Secondly, the morphotypes included in overall vegetation analysis differ between our study and previous interpretations. Zucol et al. (2010) and Bellosi et al. (2021) assessed grass biomass based not only on GSSCPs, but also on other morphotypes, including elongates (e.g., Fig. 4H), Acute bulbosus, and Bulliform flabelate to assess grass biomass, thereby augmenting the representation of grasses. In contrast, we do not include these non-GSSCP morphotypes in our vegetation analyses, because many of these forms can be produced by diverse other plant taxa, including palms or other monocots (e.g., Piperno, 2006; Neumann et al., 2019). In addition, their production has been linked to factors such as evapotranspiration rates, rather than biomass, although the relationship has proven complex (Piperno, 1993; Bremond et al., 2005, 2008; Madella et al., 2009; Jenkins et al., 2020; D'Agostini et al., 2025).

We believe these key differences in laboratory and counting approaches overrepresent grass abundances in previous studies, which, combined with abundant palm phytoliths, led Bellosi et al. (2021) to interpret late Eocene vegetation in the Gran Barranca Member of the Sarmiento Formation as palm savannas analogous to modern-day palm and grass-dominated

Chaco District vegetation in eastern Argentina (Cabrera, 1971), and savannas emerging in the late Eocene Puesto Almendra Inferior member. The scarcity of GSSCPs in the assemblages do not agree with this interpretation and are better aligned with other regional paleobotanical records (e.g., Barreda and Palazzesi, 2007; Palazzesi and Barreda, 2012).

The presence of dung beetle brood balls in the middle to late Eocene deposits of the Koluel-Kaike Formation and Gran Barranca Member of the Sarmiento Formation has also been seen as evidence for grassland environments, primarily due to the presence of GSSCPs in their phytolith content and modern dung beetle habitat preferences (Bellosi et al., 2021). However, GSSCPs are uncommon in phytolith assemblages extracted from these brood balls (Sánchez et al., 2010), indicating that grasses were rare in the diets of the dung producers and the habitat in which they were deposited (Strömberg, 2011); further, under the morphotype classification system used in this study, GSSCPs from dung beetle balls correspond to pooid grasses, not PACMADs, consistent with our results (Figs. 4D–4F; see also discussion in Strömberg et al., 2013). While dung beetle assemblages are more abundant and species-rich in African savannas than in forests (Kunz and Krell, 2011), the opposite pattern is observed today in the Neotropics, where forests support greater dung beetle richness and abundance than savannas (Estrada and Coates-Estrada, 2002; Vulinec, 2002; Kunz and Krell, 2011). This contrast has been proposed as the legacy of Pleistocene megafaunal extinctions in the Americas, which impacted open habitats more severely than closed ones (Halffter, 1991; Galetti et al., 2018), but, to our knowledge, this hypothesis has yet to be formally tested.

Early Eocene Forest Expansion

Our new spatially and temporally resolved record of vegetation change over the first 20 million years of the Cenozoic, coupled with the assemblage data of Strömberg et al. (2013), documents major temporal changes in vegetation composition, diversity, and structure through the first $\sim$45 million years of the Cenozoic. Palm phytoliths dominate early Paleocene Banco Negro Inferior phytolith assemblages, consistent with abundant palm pollen across northern and central Patagonia and warm, wet conditions that stabilized mangrove communities in coastal plain swamps (Feruglio, 1949; Barreda and Palazzesi, 2007; Comer et al., 2015). Palm content decreased during a sedimentological transition to fully fluvial environments in the Río Chico Group through the Transitional Beds (Fig. 4). In

the early Eocene, woody dicots and other FIs had become abundant (>50% of diagnostic counts) relative to palms in most assemblages across the SJB (Fig. 4). The most compositionally heterogeneous assemblages of the Río Chico Group appear leading up to the EECO in the Las Flores Formation, coeval with the highest estimated floral diversity in Cenozoic Patagonia (Woodburne et al., 2014). Palynofloras and macrofossil floras across Patagonia similarly indicate highly diverse megathermal humid forests of mixed Neotropical and Gondwanan composition (Wilf et al., 2005; Barreda and Palazzesi, 2007; Iglesias et al., 2007; Palazzesi and Barreda, 2007; Raigemborn et al., 2009).

The significant expansion of tropical biomes reflected in the early Eocene Las Flores Formation is associated with peak diversity of eutherian (placental) and metatherian (marsupial and relatives) mammals (Goin et al., 2016; Goin and Martin, 2022). The earliest records of xenarthrans (armadillo, anteater, and tree sloth relatives) in Patagonia are from the Las Flores Formation and occur concurrently with an explosive radiation of South American native ungulates (e.g., Notoungulata) as recorded in various localities and facies of the Las Flores Formation, including the Las Flores and Estancia Las Violetas localities (López et al., 2020).

The warmest period of the Eocene, the EECO, lacks well-preserved phytoliths. Abundant organic matter may have suppressed phytolith preservation during an interval of increased productivity and low sedimentation rates, as evidenced by paleosols (e.g., Ultisol- and Plinthitic Ultisol–like paleosols) in the Laguna Manantiales section (Bennett and Siegel, 1987; Strömberg et al., 2018; Raigemborn et al., 2022). The sampled beds represent B or C soil horizons, which tend to have lower concentration of phytoliths, and thus recovery would be lacking; however, previous work has found that these deeper soil horizons often have phytoliths of comparable preservation, even if not as abundant (Miller et al., 2012; Strömberg et al., 2018). Thus, the sampling strategy is unlikely to be the reason for poor recovery in this interval.

By the early–middle Eocene following the EECO, proportions of FIs decreased across the studied sections, falling to <25% in the Laguna Manantiales and Estancia Las Violetas localities. This decrease in FIs correlates with decreasing global temperatures (Fig. 4O) and a decrease in thermophilic taxa in coeval paleobotanical records in Patagonia (Barreda and Palazzesi, 2007; Rossetto-Harris and Wilf, 2024). FI composition heterogeneity also declined (albeit based on a limited sample size) between the Las Flores and Koluel-Kaike formations (Fig. 4), suggesting an increasingly homogeneous vegetation in the SJB. This potential decline in diversity could signal, as suggested in previous studies, an increasingly endemic southern South American vegetation as the opening of the Drake Passage severed biogeographic connections between South America and Australasia via Antarctica (Gandolfo et al., 2011; Carvalho et al., 2013; Wilf et al., 2013; Kooyman et al., 2014; Reguero et al., 2014; Rossetto-Harris et al., 2020; Gao et al., 2025), and Neotropical taxa abundance started to decline in southern South America (Barreda and Palazzesi, 2007; Jaramillo and Cárdenas, 2013).

In the Koluel-Kaike Formation, in contrast to the decrease in FIs at Laguna Manantiales during the middle Eocene, FIs became increasingly abundant at the Las Flores locality (Fig. 4O). It is possible that facies and environmental differences drove this disparate trend. However, given the apparent compositional homogeneity of FI assemblages across space and time in the Koluel-Kaike Formation (Fig. 5B), we favor an alternative explanation whereby the disparity is instead a result of inaccurate age model predictions for samples near the top of the Laguna Manantiales section, where fewer age constraints are available relative to the Las Flores locality. This hypothesis is supported by paleopedological studies, which infer consistent mean annual temperature and mean annual precipitation for the Koluel-Kaike Formation in the areas of the Las Flores and Laguna Manantiales localities (Krause et al., 2010; Raigemborn et al., 2018, 2022); thus, the top of the Laguna Manantiales section may be older than 45 Ma (Raigemborn et al., 2022). Further dating efforts, particularly in Laguna Manantiales, are needed to fully evaluate the influence of the age model on our results.

Rise of Open Habitats, Then Return of Forests

Our reanalysis of Sarmiento Formation phytolith records in the Las Flores and Gran Barranca localities sheds new light on ensuing middle Eocene–early Miocene vegetation changes in the SJB. This section hosts a rich record of phytoliths, reconstructed Leaf Area Index, stable isotopes, faunas, and sedimentology (Bellosi, 2010; Bellosi et al., 2010; Carlini et al., 2010; Dunn et al., 2013; Strömberg et al., 2013; Dunn et al., 2015; Kohn et al., 2015), which have been interpreted to show a shift toward increasingly open, arid habitats in the form of dry-adapted shrublands where presumably low-growing palms played a dominant role (Dunn et al., 2015; Kohn et al., 2015).

Palms gradually increased in abundance between ca. 37.5 Ma and ca. 35 Ma, reaching a maximum across the EOT (Strömberg et al., 2013; Kohn et al., 2015). This shift was potentially linked to an increase in the intensity and frequency of wildfires (Fig. 4O, Strömberg et al., 2013; Selkin et al., 2015). Nonetheless, FI compositions remained relatively homogeneous from the latest Eocene to the early Oligocene. Pollen and macrofloral records, which are biased toward woody dicots and conifers, show a gradual change in plant community composition toward an increasingly cold and arid-adapted vegetation during this time and the expansion of *Nothofagus* (southern Beech) forests, but no abrupt shifts across the EOT boundary (Barreda and Palazzesi, 2007; Quattrocchio et al., 2013).

Because macrofloras, palynofloras, and phytolith assemblages are preserved in different contexts and capture different spatial resolutions (e.g., Strömberg et al., 2018), we propose that the seemingly contrasting vegetation trends inferred from these complementary sources of paleobotanical data might signal landscape heterogeneity. That is, whereas certain areas—perhaps uplands or coastal areas—remained forested, open, woody vegetation expanded in the lowlands, increasingly so toward the end of the Eocene and into the Oligocene, even as the composition of the woody components appeared not to have changed significantly as seen in the phytolith record analyzed herein. The absence of substantial vegetation change across the EOT aligns with $\delta^{18}O$ records that suggest that unlike in the Northern Hemisphere (Zanazzi et al., 2007; Hren et al., 2013), no significant cooling occurred in Patagonia at this transition (Kohn et al., 2015). Note, however, that the temperature history across the EOT is controversial, as at least one clumped isotope record from the Southern Ocean shows no resolvable temperature decrease ($0.4 \pm 1.1\ °C$; Petersen and Schrag, 2015), while a hydrogen isotope record from Gran Barranca suggests a decrease of $5 \pm 1\ °C$ (Colwyn and Hren, 2019).

Against this background of potentially merely gradual alterations in regional temperatures and increasing aridification, faunal records show that South American mammal communities experienced significant taxonomic and ecological changes after the early Eocene, including marked shifts across the EOT. Metatherian diversity decreased dramatically between the Eocene and Oligocene, and surviving lineages experienced significant ecological turnover, by which fruit-eating taxa declined and, concurrently, grain and seed-eating taxa increased (Goin et al., 2016). Starting in the middle Eocene, South American native ungulates evolved high-crowned (hypsodont) or ever-growing (hypselodont) molars, den-

tal adaptations to abrasive items, including dietary grit (e.g., Damuth and Janis, 2011; Strömberg et al., 2013; Kohn et al., 2015; Goin et al., 2016; Goin and Martin, 2022). In parallel, ungulates with low-crowned teeth adapted for softer foods (e.g., tree leaves) disappeared from Patagonia, becoming confined to lower latitudes in South America. In addition to taxonomic turnover, the EOT reveals a trend toward increased body mass in South American native ungulates like Astrapotheria, Notoungulata, and Pyrotheria (Croft et al., 2020). Many of these changes were initially interpreted as responses to cooler climates but are also consistent with adaptations to increasingly open, arid (but relatively warm) habitats and the loss of forests with ample supply of, for example, fruits (e.g., Dunn et al., 2015; Kohn et al., 2015; Chen et al., 2019).

Records from the Colhue Huapi Member at Gran Barranca show that, by the early Miocene, the composition and heterogeneity of FI assemblages rebounded to become broadly similar to those of the Gran Barranca Member (Figs. 5A and 6). FI phytoliths increased (Fig. 4O), and open-habitat grasses expanded at the expense of palms (Strömberg et al., 2013). Reconstructed Leaf Area Index indicates the reappearance of relatively closed lowland habitats (e.g., broadleaf forests, although alternating with grassy patches; Dunn et al., 2015). Stable C isotopic data indicate that regional rainfall levels increased toward the early Miocene (Kohn et al., 2015; Trayler et al., 2020), perhaps allowing for a more closed canopy overall, at least initially. These combined records point to more locally heterogeneous vegetation, both in terms of composition and structure, relative to the late Eocene and early Oligocene. Our data and interpretations agree with other paleobotanical data from Patagonia that suggest a re-emergence of megathermal, yet more xerophytic, communities in the lead-up to the warmer and wetter climates of the middle Miocene (Barreda and Palazzesi, 2007; Palazzesi and Barreda, 2007; Trayler et al., 2020).

Non-Analog Ecologies Characterized South American Plant Communities

Emerging reconstructions of ancient Patagonian ecosystems strongly suggest non-analog ecological associations of important plant functional types and faunas. For example, Pooideae today are predominantly cold- and dry-tolerant (Edwards and Smith, 2010; Schubert et al., 2019). In contrast, members of Pooideae occur in the Las Flores Formation of the Laguna Manantiales assemblages of the early Eocene, when Patagonian paleoclimates were signifi-

cantly warmer and wetter than today (Wilf et al., 2005; Palazzesi and Barreda, 2007), and abundant palm phytoliths indicate frost-free climates (e.g., Wing and Greenwood, 1993; Reichgelt et al., 2018; Brightly et al., 2024). This Pooideae–Arecaceae (palm) association, which has also been observed in, for example, the middle Miocene lowlands of Bolivia (Strömberg et al., 2024), could suggest that either palms or Pooideae had a broader climatic tolerance range in the past. Based on the documentation of thermophilic taxa in the Eocene of Patagonia (Palazzesi and Barreda, 2007), the latter is more likely.

Although we cannot yet reliably infer the paleoecology of ancient palms based on phytolith morphology alone (Brightly et al., 2024), the dominance of palms in Eocene–Miocene shrublands potentially maintained by episodic wildfire activity (Selkin et al., 2015) suggests that their niche space may have also been non-analog. Many modern palm species are resistant to or adapted to fire (McPherson and Williams, 1998; Souza and Martins, 2004; Liesenfeld, 2025), but palm-dominated vegetation today typically experiences infrequent burning (McPherson and Williams, 1998). Broader environmental tolerances of extinct taxa compared to their modern relatives could have facilitated the establishment of non-analog mixed tropical-Antarctic paleofloras during the early Cenozoic, in the context of regional climate systems only possible before the rise of the Andes (Hinojosa and Villagrán, 2005). Today, areas with palm-dominated vegetation in southern South America are characterized by a continuous C_4 PACMAD grass understory (Cabrera, 1971; Sosinski et al., 2019; see also discussion in Strömberg et al., 2024), yet we see no PACMADs in our phytolith assemblages.

Other studies have struggled to interpret paleobotanical assemblages in the Cenozoic of Patagonia, given their inferred non-analogous vegetation structure (Dunn et al., 2015) and composition, which includes a mix of Neotropical and Antarctic lineages resulting in the so-called "mixed paleofloras" (e.g., Romero, 1986; Iglesias et al., 2007; Hinojosa and Villagrán, 2005; Wilf et al., 2013; Hinojosa et al., 2016). These compositional differences were possibly accompanied (or driven) by alterations in plant physiological functions (e.g., drought tolerance) relative to today, due to the elevated temperatures and pCO_2 levels of the early Cenozoic (Kohn et al., 2015; Hinojosa et al., 2016); however, this hypothesis remains untested.

Like floras, faunal communities in Patagonia were neither functionally nor compositionally analogous to any extant community in South America or elsewhere, particularly during the

emergence of highly endemic early Paleogene communities. These communities were characterized by a remarkable diversity of non-therian and therian mammals (Pascual and Ortiz-Jaureguizar, 2007) and were dominated by herbivorous forms like South American native ungulates (Croft et al., 2020). In contrast, few mammals with carnivorous diets were recorded. Instead, birds, crocodilians, and large snakes likely assumed the primary predatory roles in these ecosystems, both in the early Eocene of Patagonia and in Antarctic localities (Croft, 2006; Woodburne et al., 2014; Gelfo et al., 2019; Croft et al., 2020; Acosta Hospitaleche and Jones, 2024). As global temperatures declined at the EOT, mammalian communities also displayed species with larger body sizes, ultimately giving rise to Miocene assemblages that lack modern analogs but are functionally more similar to those found in Southeast Asia and Africa (Catena and Croft, 2020).

CONCLUSIONS

We present the first basin-wide Paleogene paleobotanical reconstruction of southern South American floras. Furthermore, we demonstrate that integrating phytolith analysis with pollen, macrofloral, sedimentological, and geochemical records yields a nuanced view of vegetation structure, composition, and climatic mechanisms in the early Cenozoic, and provides an evolutionary context for the highly endemic South American faunas of the early Cenozoic. Taken together, paleobotanical records of the SJB suggest that warm and humid forests covering southern South America in the Paleocene–early Eocene transitioned into more open, arid shrublands in the Patagonian lowlands by the middle to late Eocene (Sarmiento Formation) as regional climates became cooler and drier. Humid megathermal forests returned by the early–middle Miocene as temperatures and precipitation increased, but open-habitat grasses also expanded, pointing to a mosaic landscape. These changes roughly track global temperatures (Zachos et al., 2001; Westerhold et al., 2020), although some local records suggest little to no temperature variation during rapid and globally significant climatic events such as the EOT (e.g., Kohn et al., 2015). In the context of previous paleobotanical work demonstrating the existence of Gondwanan connections in Eocene macrofloras of Patagonia (Wilf et al., 2005; Raigemborn et al., 2009; Gandolfo et al., 2011; Kooyman et al., 2014; Rossetto-Harris et al., 2020), and the increased dissimilarity between Neotropical and southern South American palynological

records during the early Eocene (Jaramillo and Cárdenas, 2013) the new Paleocene–early Eocene SJB phytolith record signals the last pulses of Antarctic, rather than Neotropical rainforest expansion, and contradicts hypotheses that grassy habitats spread in early Cenozoic of southern South America.

The incomplete yet ecologically diverse fossil record of Antarctic mammals, currently restricted to the Eocene La Meseta and Submeseta formations on Seymour/Marambio Island, provides some support for the notion of forest expansions across the southern part of the Gondwana continents during this time. For example, the largest Antarctic mammals (>10 kg) of the South American native ungulates (Astrapotheria and Sparnotheriodontidae) have browsing specializations characteristic of forest-dwelling mammals (Gelfo et al., 2019). Antarctic metatherians (<1 kg) were likely adapted to processing relatively hard food items, including seeds, specific types of fruits, and insects with rigid exoskeletons, while some marsupials were strict fruit or leaf-eaters, all pointing to forested environments (Chen et al., 2019; Goin et al., 2020).

Understanding the history of South American vegetation is vital for inferring what mechanisms and circumstances dictated its origin (e.g., Hoorn et al., 2010). It is also key for inferring what processes drove Cenozoic faunal evolution because vegetation structure and composition directly influence the availability of habitats and resources (e.g., Chen et al., 2019). For example, in southern South America, browsing mammal diversity peaked in the early Paleogene when paleobotanical evidence suggests closed forests, followed by a decline during the Eocene–early Oligocene as herbivores adapted to the increasingly open habitats with abundant abrasive particles, notably decoupled from the later rise of grassy habitats (Ortiz-Jaureguizar and Cladera, 2006; Strömberg et al., 2013; Dunn et al., 2015; Kohn et al., 2015). Future research prioritizing the integration of floral and faunal records in local and global climatic contexts will enhance our understanding of past ecosystem assembly and function and better predict how modern ecosystems may respond to ongoing environmental changes.

REFERENCES CITED

Acosta Hospitaleche, C., and Jones, W., 2024, Insights on the oldest terror bird (Aves, Phorusrhacidae) from the Eocene of Argentina: Historical Biology, v. 37, p. 391–399, https://doi.org/10.1080/08912963.2024.2304592.

Andreis, R.R., 1977, Geología del area de Cañadón Hondo, Depto. Escalante, Provincia del Chubut: Republica Argentina: Obra del Centenario del Museo de La Plata, v. 4, p. 77–102.

Barnosky, A.D., et al., 2017, Merging paleobiology with conservation biology to guide the future of terrestrial ecosystems: Science, v. 355, https://doi.org/10.1126/science.aah4787.

Barreda, V., and Palazzesi, L., 2007, Patagonian vegetation turnovers during the Paleogene–early Neogene: Origin of arid-adapted floras: Botanical Review, v. 73, p. 31–50, https://doi.org/10.1663/0006-8101(2007)73[31:PVTDTP]2.0.CO;2.

Barreda, V.D., and Palazzesi, L., 2010, Vegetation during the Eocene–Miocene interval in central Patagonia: A context of mammal evolution, in Madden, R.H., Carlini, A.A., Vucetich, M.G., and Kay, R.F., eds., The Paleontology of Gran Barranca: Evolution and Environmental Change through the Middle Cenozoic of Patagonia: Cambridge, UK, Cambridge University Press, p. 371–278.

Barreda, V.D., Zamaloa, M. del C., Gandolfo, M.A., Jaramillo, C., and Wilf, P., 2020, Early Eocene spore and pollen assemblages from the Laguna del Hunco fossil lake beds, Patagonia, Argentina: International Journal of Plant Sciences, v. 181, p. 594–615, https://doi.org/10.1086/708386.

Bellosi, E.S., 2010, Loessic and fluvial sedimentation in Sarmiento Formation pyroclastics, middle Cenozoic of central Patagonia, in Madden, R.H., Carlini, A.A., Vucetich, M.G., and Kay, R.F., eds., The Paleontology of Gran Barranca: Evolution and Environmental Change through the Middle Cenozoic of Patagonia: Cambridge, UK, Cambridge University Press, p. 278–292.

Bellosi, E.S., and Krause, J.M., 2014, Onset of the middle Eocene global cooling and expansion of open-vegetation habitats in Central Patagonia: Andean Geology, v. 41, https://doi.org/10.5027/andgeoV41n1-a02.

Bellosi, E.S., Laza, J.H., Sánchez, M.V., and Genise, J., 2010, Ichnofacies analysis of the Sarmiento Formation (middle Eocene–early Miocene) at Gran Barranca, central Patagonia, in Madden, R.H., Carlini, A.A., Vucetich, M.G., and Kay, R.F., eds., The Paleontology of Gran Barranca: Evolution and Environmental Change through the Middle Cenozoic of Patagonia: Cambridge, UK, Cambridge University Press, p. 306–316.

Bellosi, E.S., Genise, J.F., Zucol, A., Bond, M., Kramarz, A., Sánchez, M.V., and Krause, J.M., 2021, Diverse evidence for grasslands since the Eocene in Patagonia: Journal of South American Earth Sciences, v. 108, https://doi.org/10.1016/j.jsames.2021.103357.

Bennett, P., and Siegel, D.I., 1987, Increased solubility of quartz in water due to complexing by organic compounds: Nature, v. 326, p. 684–686, https://doi.org/10.1038/326684a0.

Black, L.P., et al., 2004, Improved [206]Pb/[238]U microprobe geochronology by the monitoring of a trace-element-related matrix effect; SHRIMP, ID-TIMS, ELA-ICP-MS and oxygen isotope documentation for a series of zircon standards: Chemical Geology, v. 205, p. 115–140, https://doi.org/10.1016/j.chemgeo.2004.01.003.

Brea, M., Zucol, A.F., Raigemborn, M.S., and Matheos, S.D., 2008, Reconstrucción de paleocomunidades arbóreas mediante análisis fitolíticos en sedimentos del Paleoceno superior-?Eoceno (Formación las Flores), Chubut, Argentina, in Korstanje, M.A., and Babot, M. del P., eds., Matices Interdisciplinarios en Estudios Fitolíticos y de Otros Microfósiles: Oxford, UK, British Archaeological Reports, p. 91–108.

Bremond, L., Alexandre, A., Peyron, O., and Guiot, J., 2005, Grass water stress estimated from phytoliths in West Africa: Journal of Biogeography, v. 32, p. 311–327, https://doi.org/10.1111/j.1365-2699.2004.01162.x.

Bremond, L., Alexandre, A., Wooller, M.J., Hély, C., Williamson, D., Schäfer, P.A., Majule, A., and Guiot, J., 2008, Phytolith indices as proxies of grass subfamilies on East African tropical mountains: Global and Planetary Change, v. 61, p. 209–224, https://doi.org/10.1016/j.gloplacha.2007.08.016.

Brightly, W.H., Crifò, C., Gallaher, T.J., Hermans, R., Lavin, S., Lowe, A.J., Smythies, C.A., Stiles, E., Wilson Deibel, P., and Strömberg, C.A.E., 2024, Palms of the past: Can morphometric phytolith analysis inform deep time evolution and palaeoecology of Arecaceae?: Annals of Botany, v. 134, https://doi.org/10.1093/aob/mcae068.

Cabrera, A.L., 1971, Fitogeografía de la República Argentina: Boletín de la Sociedad Argentina de Botánica, v. 14, p. 1–42.

Carlini, A.A, Ciancio, M.R, and Scillato-Yané, G.J., 2010, Middle Eocene–early Miocene Dasypodidae (Xenarthra) of southern South America: Faunal succession at Gran, in Madden, R.H., Carlini, A.A., Vucetich, M.G., and Kay, R.F., eds., The Paleontology of Gran Barranca: Evolution and Environmental Change through the Middle Cenozoic of Patagonia: Cambridge, UK, Cambridge University Press, p. 106–129.

Carvalho, M.R., Wilf, P., Hermsen, E.J., Gandolfo, M.A., Cúneo, N.R., and Johnson, K.R., 2013, First record of Todea (Osmundaceae) in South America, from the early Eocene paleorainforests of Laguna del Hunco (Patagonia, Argentina): American Journal of Botany, v. 100, p. 1831–1848, https://doi.org/10.3732/ajb.1200637.

Catena, A.M., and Croft, D.A., 2020, What are the best modern analogs for ancient South American mammal communities? Evidence from ecological diversity analysis (EDA): Palaeontologia Electronica, v. 23, p. 1–36, https://doi.org/10.26879/962.

Chen, M., Strömberg, C.A.E., and Wilson, G.P., 2019, Assembly of modern mammal community structure driven by Late Cretaceous dental evolution, rise of flowering plants, and dinosaur demise: Proceedings of the National Academy of Sciences of the United States of America, v. 116, p. 9931–9940, https://doi.org/10.1073/pnas.1820863116.

Cleveland, W.S., and Devlin, S.J., 1988, Locally weighted regression: An approach to regression analysis by local fitting: Journal of the American Statistical Association, v. 83, p. 596–610, https://doi.org/10.1080/01621459.1988.10478639.

Clyde, W.C., et al., 2014, New age constraints for the Salamanca Formation and lower Río Chico Group in the western San Jorge Basin, Patagonia, Argentina: Implications for Cretaceous-Paleogene extinction recovery and land mammal age correlations: Geological Society of America Bulletin, v. 126, p. 289–306, https://doi.org/10.1130/B30915.1.

Colwyn, D.A., and Hren, M.T., 2019, An abrupt decrease in Southern Hemisphere terrestrial temperature during the Eocene–Oligocene transition: Earth and Planetary Science Letters, v. 512, p. 227–235, https://doi.org/10.1016/j.epsl.2019.01.052.

Comer, E.E., Slingerland, R.L., Krause, J.M., Iglesias, A., Clyde, W.C., Raigemborn, M.S., and Wilf, P., 2015, Sedimentary facies and depositional environments of diverse Early Paleocene floras, north-central San Jorge

Basin, Patagonia, Argentina: PALAIOS, v. 30, p. 553–573, https://doi.org/10.2110/palo.2014.064.

Crifò, C., and Strömberg, C.A.E., 2021, Spatial patterns of soil phytoliths in a wet vs. dry neotropical forest: Implications for paleoecology: Palaeogeography, Palaeoclimatology, Palaeoecology, v. 562, https://doi.org/10.1016/j.palaeo.2020.110100.

Croft, D.A., 2006, Do marsupials make good predators? Insights from predator-prey diversity ratios: Evolutionary Ecology Research, v. 8, p. 1193–1214.

Croft, D.A., Gelfo, J.N., and López, G.M., 2020, Splendid innovation: The extinct South American native ungulates: Annual Review of Earth and Planetary Sciences, v. 48, p. 259–290, https://doi.org/10.1146/annurev-earth-072619-060126.

D'Agostini, F., Ruiz Pérez, J., Madella, M., Vadez, V., and Lancelotti, C., 2025, Predicting plant water availability from phytolith assemblages: An experimental approach for archaeological reconstructions in drylands: Vegetation History and Archaeobotany, v. 34, p. 239–255, https://doi.org/10.1007/s00334-024-01012-9.

Damuth, J., and Janis, C.M., 2011, On the relationship between hypsodonty and feeding ecology in ungulate mammals, and its utility in palaeoecology: Biological Reviews of the Cambridge Philosophical Society, v. 86, p. 733–758, https://doi.org/10.1111/j.1469-185X.2011.00176.x.

Dickau, R., Whitney, B.S., Iriarte, J., Mayle, F.E., Soto, J.D., Metcalfe, P., Street-Perrott, F.A., Loader, N.J., Ficken, K.J., and Killeen, T.J., 2013, Differentiation of neotropical ecosystems by modern soil phytolith assemblages and its implications for palaeoenvironmental and archaeological reconstructions: Review of Palaeobotany and Palynology, v. 193, p. 15–37, https://doi.org/10.1016/j.revpalbo.2013.01.004.

Dunn, R.E., Madden, R.H., Kohn, M.J., Schmitz, M.D., Strömberg, C.A.E., Carlini, A.A., Ré, G.H., and Crowley, J., 2013, A new chronology for middle Eocene–early Miocene South American Land Mammal Ages: Geological Society of America Bulletin, v. 125, p. 539–555, https://doi.org/10.1130/B30660.1.

Dunn, R.E., Strömberg, C.A.E., Madden, R.H., Kohn, M.J., and Carlini, A.A., 2015, Linked canopy, climate, and faunal change in the Cenozoic of Patagonia: Science, v. 347, p. 258–261, https://doi.org/10.1126/science.1260947.

Edwards, E.J., and Smith, S.A., 2010, Phylogenetic analyses reveal the shady history of C$_4$ grasses: Proceedings of the National Academy of Sciences, v. 107, p. 2532–2537, https://doi.org/10.1073/pnas.0909672107.

Estrada, A., and Coates-Estrada, R., 2002, Dung beetles in continuous forest, forest fragments and in an agricultural mosaic habitat island at Los Tuxtlas, Mexico: Biodiversity and Conservation, v. 11, p. 1903–1918, https://doi.org/10.1023/A:1020896928578.

Feruglio, E., 1949, Descripción geológica de la Patagonia, vol I: Buenos Aires, Argentina, Ministerio de la Industria y el Comercio de la Nación.

Fitzgerald, M.G., Mitchum, R.M., Jr., Uliana, M.A., and Biddle, K.T., 1990, Evolution of the San Jorge Basin, Argentina: AAPG Bulletin, v. 74, p. 879–920, https://doi.org/10.1306/0C9B23C1-1710-11D7-8645000102C1865D.

Galetti, M., et al., 2018, Ecological and evolutionary legacy of megafauna extinctions: Biological Reviews of the Cambridge Philosophical Society, v. 93, p. 845–862, https://doi.org/10.1111/brv.12374.

Gandolfo, M.A., Hermsen, E.J., Zamaloa, M.C., Nixon, K.C., Gonzalez, C.C., Wilf, P., Cuneo, N.R., and Johnson, K.R., 2011, Oldest known Eucalyptus macrofossils are from South America: PLoS One, v. 6, https://doi.org/10.1371/journal.pone.0021084.

Gao, L., et al., 2025, The initial opening of the drake passage occurred during ca. 62–59 Ma: Geophysical Research Letters, v. 52, https://doi.org/10.1029/2024GL111455.

Gelfo, J.N., Goin, F.J., Bauzá, N., and Reguero, M.A., 2019, The fossil record of Antarctic land mammals: Commented review and hypotheses for future research: Advances in Polar Science, v. 30, p. 274–292, https://doi.org/10.13679/j.advps.2019.0021.

Goin, F.J., and Martin, G., 2022, Cenozoic South American Metatherians (Mammalia, Theria) as indicators of climate–environmental changes, *in* Larramendy,

M.L., and Liwszyc, G., eds., Marsupial and Placental Mammal Species in Environmental Risk Assessment Strategies: The Royal Society of Chemistry, Issues in Toxicology Series, p. 9–46, https://doi.org/10.1039/9781839163470-00009.

Goin, F., Woodburne, M., Zimicz, A.N., Martin, G.M., and Chornogubsky, L., 2016, A Brief History of South American Metatherians—Evolutionary Contexts and Intercontinental Dispersals: Dordrecht, Netherlands, Springer Earth System Sciences, 237 p., https://doi.org/10.1007/978-94-017-7420-8.

Goin, F.J., Vieytes, E.C., Gelfo, J.N., Chornogubsky, L., Zimicz, A.N., and Reguero, M.A., 2020, New metatherian mammal from the Early Eocene of Antarctica: Journal of Mammalian Evolution, v. 27, p. 17–36, https://doi.org/10.1007/s10914-018-9449-6.

Halffter, G., 1991, Historical and ecological factors determining the geographical distribution of beetles (Coleoptera: Scarabaeidae: Scarabaeinae): The Journal of Integrative Biogeography, v. 15, p. 11–40, https://doi.org/10.21426/B615110376.

Haslett, J., and Parnell, A., 2008, A simple monotone process with application to radiocarbon-dated depth chronologies: Journal of the Royal Statistical Society, Series C: Applied Statistics, v. 57, p. 399–418, https://doi.org/10.1111/j.1467-9876.2008.00623.x.

Hinojosa, L.F., and Villagrán, C., 2005, Did South American mixed paleofloras evolve under thermal equability or in the absence of an effective Andean barrier during the Cenozoic?: Palaeogeography, Palaeoclimatology, Palaeoecology, v. 217, p. 1–23, https://doi.org/10.1016/j.palaeo.2004.11.013.

Hinojosa, L.F., et al., 2016, Non-congruent fossil and phylogenetic evidence on the evolution of climatic niche in the Gondwana genus Nothofagus: Journal of Biogeography, v. 43, p. 555–567, https://doi.org/10.1111/jbi.12650.

Hoorn, C., et al., 2010, Amazonia through time: Andean uplift, climate change, landscape evolution, and biodiversity: Science, v. 330, p. 927–931, https://doi.org/10.1126/science.1194585.

Hren, M.T., Sheldon, N.D., Grimes, S.T., Collinson, M.E., Hooker, J.J., Bugler, M., and Lohmann, K.C., 2013, Terrestrial cooling in Northern Europe during the Eocene–Oligocene transition: Proceedings of the National Academy of Sciences of the United States of America, v. 110, p. 7562–7567, https://doi.org/10.1073/pnas.1210930110.

Ibañez-Mejia, M., and Tissot, F.L.H., 2019, Extreme Zr stable isotope fractionation during magmatic fractional crystallization: Science Advances, v. 5, https://doi.org/10.1126/sciadv.aax8648.

Iglesias, A., Wilf, P., Johnson, K.R., Cuneo, N.R., and Matheos, S.D., 2007, A Paleocene lowland macroflora from Patagonia reveals significantly greater richness than North American analogs: Geology, v. 35, p. 947–950, https://doi.org/10.1130/G23889A.1.

Iglesias, A.R.I., Artabe, A.E., and Morel, E.M., 2011, The evolution of Patagonian climate and vegetation from the Mesozoic to the present: Biological Journal of the Linnean Society, v. 103, p. 409–422, https://doi.org/10.1111/j.1095-8312.2011.01657.x.

Iriarte, J., and Paz, E.A., 2009, Phytolith analysis of selected native plants and modern soils from southeastern Uruguay and its implications for paleoenvironmental and archeological reconstruction: Quaternary International, v. 193, p. 99–123, https://doi.org/10.1016/j.quaint.2007.10.008.

Jaramillo, C., 2023, The evolution of extant South American tropical biomes: The New Phytologist, v. 239, p. 477–493, https://doi.org/10.1111/nph.18931.

Jaramillo, C., and Cárdenas, A., 2013, Global warming and neotropical rainforests: A historical perspective: Annual Review of Earth and Planetary Sciences, v. 41, p. 741–766, https://doi.org/10.1146/annurev-earth-042711-105403.

Jenkins, E.L., Predanich, L., Al Nuimat, S.A.M.Y., Jamjoum, K.I., and Stafford, R., 2020, Assessing past water availability using phytoliths from the C$_4$ plant *Sorghum bicolor*: An experimental approach: Journal of Archaeological Science: Reports, v. 33, https://doi.org/10.1016/j.jasrep.2020.102460.

Kohn, M.J., Strömberg, C.A.E., Madden, R.H., Dunn, R.E., Evans, S., Palacios, A., and Carlini, A.A., 2015, Quasistatic Eocene–Oligocene climate in Patagonia promotes slow faunal evolution and mid-Cenozoic global cooling: Palaeogeography, Palaeoclimatology, Palaeoecology, v. 435, p. 24–37, https://doi.org/10.1016/j.palaeo.2015.05.028.

Kooyman, R.M., et al., 2014, Paleo-Antarctic rainforest into the modern old world tropics: The rich past and threatened future of the "southern wet forest survivors": American Journal of Botany, v. 101, p. 2121–2135, https://doi.org/10.3732/ajb.1400340.

Krause, J.M., Bellosi, E.S., and Raigemborn, M.S., 2010, Lateritized tephric palaeosols from central Patagonia, Argentina: A southern high-latitude archive of Palaeogene global greenhouse conditions: Sedimentology, v. 57, p. 1721–1749, https://doi.org/10.1111/j.1365-3091.2010.01161.x.

Krause, J.M., Clyde, W.C., Ibáñez-Mejía, M., Schmitz, M.D., Barnum, T., Bellosi, E.S., and Wilf, P., 2017, New age constraints for early Paleogene strata of central Patagonia, Argentina: Implications for the timing of South American Land Mammal Ages: Geological Society of America Bulletin, v. 129, p. 886–903, https://doi.org/10.1130/B31561.1.

Kunz, B.K., and Krell, F., 2011, Habitat differences in dung beetle assemblages in an African savanna–forest ecotone: Implications for secondary seed dispersal: Integrative Zoology, v. 6, p. 81–96, https://doi.org/10.1111/j.1749-4877.2011.00240.x.

Legarreta, L., and Uliana, M.A., 1994, Asociaciones de fósiles y hiatos en el Supracretácico-Neógeno de Patagonia: Una perspectiva estratigrafo-secuencial: Ameghiniana, v. 31, p. 257–281.

Liesenfeld, M.V.d.A., 2025, Revealing the impact of understory fires on stem survival in palms (Arecaceae): An experimental approach using predictive models: Fire, v. 8, https://doi.org/10.3390/fire8010002.

López, G.M., Gelfo, J.N., Bauzá, N., Bond, M., and Tejedor, M.F., 2020, Biochron and diversity of Archaeopithecidae (Mammalia, Notoungulata) and a new genus and species from the Eocene of Patagonia, Argentina: Ameghiniana, v. 57, p. 103–116, https://doi.org/10.5710/AMGH.18.01.2020.3291.

Macdonald, F.A., Schmitz, M.D., Strauss, J.V., Halverson, G.P., Gibson, T.M., Eyster, A., Cox, G., Mamrol, P., and Crowley, J.L., 2018, Cryogenian of Yukon: Precambrian Research, v. 319, p. 114–143, https://doi.org/10.1016/j.precamres.2017.08.015.

Madella, M., Jones, M.K., Echlin, P., Powers-Jones, A., and Moore, M., 2009, Plant water availability and analytical microscopy of phytoliths: Implications for ancient irrigation in arid zones: Quaternary International, v. 193, p. 32–40, https://doi.org/10.1016/j.quaint.2007.06.012.

McPherson, K., and Williams, K., 1998, Fire resistance of cabbage palms (Sabal palmetto) in the southeastern USA: Forest Ecology and Management, v. 109, p. 197–207, https://doi.org/10.1016/S0378-1127(98)00243-6.

Miller, L.A., Smith, S.Y., Sheldon, N.D., and Strömberg, C.A.E., 2012, Eocene vegetation and ecosystem fluctuations inferred from a high-resolution phytolith record: Geological Society of America Bulletin, v. 124, p. 1577–1589, https://doi.org/10.1130/B30548.1.

Neumann, K., Strömberg, C.A.E., Ball, T., Albert, R.M., Vrydaghs, L., and Cummings, L.S., 2019, International Code for Phytolith Nomenclature (ICPN) 2.0: Annals of Botany, v. 124, p. 189–199, https://doi.org/10.1093/aob/mcz064.

Ortiz-Jaureguizar, E., and Cladera, G.A., 2006, Paleoenvironmental evolution of southern South America during the Cenozoic: Journal of Arid Environments, v. 66, p. 498–532, https://doi.org/10.1016/j.jaridenv.2006.01.007.

Palazzesi, L., and Barreda, V., 2007, Major vegetation trends in the Tertiary of Patagonia (Argentina): A qualitative paleoclimatic approach based on palynological evidence: Flora, v. 202, p. 328–337, https://doi.org/10.1016/j.flora.2006.07.006.

Palazzesi, L., and Barreda, V., 2012, Fossil pollen records reveal a late rise of open-habitat ecosystems in Patagonia: Nature Communications, v. 3, p. 1294–1296, https://doi.org/10.1038/ncomms2299.

Pascual, R., and Ortiz-Jaureguizar, E., 2007, The Gondwanan and South American episodes: Two major and unrelated moments in the history of the South American mammals: Journal of Mammalian Evolution, v. 14, p. 75–137, https://doi.org/10.1007/s10914-007-9039-5.

Peppe, D.J., et al., 2023, Oldest evidence of abundant C_4 grasses and habitat heterogeneity in eastern Africa: Science, v. 380, p. 173–177, https://doi.org/10.1126/science.abq2834.

Petersen, S.V., and Schrag, D.P., 2015, Antarctic ice growth before and after the Eocene-Oligocene transition: New estimates from clumped isotope paleothermometry: Paleoceanography, v. 30, p. 1305–1317, https://doi.org/10.1002/2014PA002769.

Piperno, D.R., 1993, Phytolith and charcoal records from deep lake cores in the American tropics, *in* Pearsall, D.M., and Piperno, D.R., eds., Current Research in Phytolith Analysis: Applications in Archaeology and Paleoecology: Philadelphia, Pennsylvania, University Museum of Archaeology and Anthropology, University of Pennsylvania, p. 59–71.

Piperno, D.R., 2006, Phytoliths: A Comprehensive Guide for Archaeologists and Paleoecologists: Lanham, Maryland, Altamira Press, 248 p.

Piperno, D.R., and McMichael, C., 2020, Phytoliths in modern plants from amazonia and the neotropics at large: Implications for vegetation history reconstruction: Quaternary International, v. 565, p. 54–74, https://doi.org/10.1016/j.quaint.2020.10.043.

Quattrocchio, M.E., Martínez, M.A., Hinojosa, L.F., and Jaramillo, C., 2013, Quantitative analysis of Cenozoic palynofloras from Patagonia, southern South America: Palynology, v. 37, p. 246–258, https://doi.org/10.1080/01916122.2013.787126.

Quattrocchio, M.E., Agüero, LS.., Iglesias, A., and Raigemborn, M.S., 2024, Palinoestratigrafía del Paleógeno temprano en la localidad de Laguna Manantiales, Sur de la Cuenca del Golfo San Jorge, Argentina: Publicación Electrónica de la Asociación Paleontológica Argentina, https://doi.org/10.5710/PEAPA.29.12.2023.491.

Raigemborn, M.S., and Beilinson, E., 2020, Stratigraphic architecture and paleosols as basin correlation tools of the early Paleogene infill in central–south Patagonia, Golfo San Jorge Basin, Argentinean Patagonia: Journal of South American Earth Sciences, v. 99, https://doi.org/10.1016/j.jsames.2020.102519.

Raigemborn, M., Brea, M., Zucol, A., and Matheos, S., 2009, Early Paleogene climate at mid latitude in South America: Mineralogical and paleobotanical proxies from continental sequences in Golfo San Jorge basin (Patagonia, Argentina): Geologica Acta, v. 7, p. 125–145, https://doi.org/10.1344/105.000000269.

Raigemborn, M.S., Krause, J.M., Bellosi, E., and Matheos, S.D., 2010, Redefinición estratigráfica del Grupo Río Chico (Paleógeno Inferior), en el norte de la cuenca del Golfo San Jorge, Chubut: Revista de la Asociación Geológica Argentina, v. 67, p. 239–256.

Raigemborn, M.S., Beilinson, E., Krause, J.M., Varela, A.N., Bellosi, E., Matheos, S.D., and Sosa, N., 2018, Paleolandscape reconstruction and interplay of controlling factors of an Eocene pedogenically-modified distal volcaniclastic succession in Patagonia: Journal of South American Earth Sciences, v. 86, p. 475–496, https://doi.org/10.1016/j.jsames.2018.07.001.

Raigemborn, M.S., Lizzoli, S., Hyland, E., Cotton, J., Gómez Peral, L.E., Beilinson, E., and Krause, J.M., 2022, A paleopedological approach to understanding Eocene environmental conditions in southern Patagonia, Argentina: Palaeogeography, Palaeoclimatology, Palaeoecology, v. 601, https://doi.org/10.1016/j.palaeo.2022.111129.

Ré, G.H., Bellosi, E.S., Heizler, M., Vilas, J.F., Madden, R.H., Carlini, A.A., Kay, R.F., and Vucetich, M.G., 2010, A geochronology for the Sarmiento Formation at Gran Barranca, *in* Madden, R.H., Carlini, A.A., Vucetich, M.G., and Kay, R.F., eds., The Paleontology of Gran Barranca: Evolution and Environmental Change through the Middle Cenozoic of Patagonia, Cambridge, UK, Cambridge University Press, p. 46–59.

Reguero, M.A., Gelfo, J.N., López, G.M., Bond, M., Abello, A., Santillana, S.N., and Marenssi, S.A., 2014, Final Gondwana breakup: The Paleogene South American native ungulates and the demise of the South American–Antarctica land connection: Global and Planetary Change, v. 123, p. 400–413, https://doi.org/10.1016/j.gloplacha.2014.07.016.

Reichgelt, T., West, C.K., and Greenwood, D.R., 2018, The relation between global palm distribution and climate: Scientific Reports, v. 8, 4721, https://doi.org/10.1038/s41598-018-23147-2.

Romero, E.J., 1986, Paleogene phytogeography and climatology of South America: Annals of the Missouri Botanical Garden, v. 73, p. 449–461, https://doi.org/10.2307/2399123.

Rossetto-Harris, G., and Wilf, P., 2024, Reassessing floral diversity at Río Pichileufú, earliest middle Eocene of Río Negro, Argentina: Palaeontologia Electronica, v. 27, a49, https://doi.org/10.26879/1383.

Rossetto-Harris, G., Wilf, P., Escapa, I.H., and Andruchow-Colombo, A., 2020, Eocene *Araucaria* Sect. *Eutacta* from Patagonia and floristic turnover during the initial isolation of South America: American Journal of Botany, v. 107, p. 806–832, https://doi.org/10.1002/ajb2.1467.

Sánchez, M.V., González, M.G., and Genise, J.F., 2010, Phytolith analysis of *Coprinisphaera*, unlocking dung beetle behaviour, herbivore diets and palaeoenvironments along the middle Eocene–early Miocene of Patagonia: Palaeogeography, Palaeoclimatology, Palaeoecology, v. 285, p. 224–236, https://doi.org/10.1016/j.palaeo.2009.11.014.

Schubert, M., Marcussen, T., Meseguer, A.S., and Fjellheim, S., 2019, The grass subfamily Pooideae: Cretaceous–Palaeocene origin and climate-driven Cenozoic diversification: Global Ecology and Biogeography, v. 28, https://doi.org/10.1111/geb.12923.

Scotese, C.R., and Dreher, C., 2012, GlobalGeology: http://www.globalgeology.com/.

Selkin, P.A., Strömberg, C.A.E., Dunn, R., Kohn, M.J., Carlini, A.A., Siân Davies-Vollum, K., and Madden, R.H., 2015, Climate, dust, and fire across the Eocene-Oligocene transition, Patagonia: Geology, v. 43, p. 567–570, https://doi.org/10.1130/G36664.1.

Soreng, R.J., et al., 2022, A worldwide phylogenetic classification of the Poaceae (Gramineae) III: An update: Journal of Systematics and Evolution, v. 60, p. 476–521, https://doi.org/10.1111/jse.12847.

Sosinski, E.E., Jr., Urruth, L.M., Barbieri, R.L., Marchi, M.M., and Gildo Martens, S., 2019, On the ecological recognition of *Butia* palm groves as integral ecosystems: Why do we need to widen the legal protection and the in situ/on-farm conservation approaches?: Land Use Policy, v. 81, p. 124–130, https://doi.org/10.1016/j.landusepol.2018.10.041.

Souza, A.F., and Martins, F.R., 2004, Population structure and dynamics of a neotropical palm in fire-impacted fragments of the Brazilian Atlantic Forest: Biodiversity and Conservation, v. 13, p. 1611–1632, https://doi.org/10.1023/B:BIOC.0000029326.44647.7f.

Spalletti, L.A., and Mazzoni, M.M., 1979, Estratigrafía de la Formación Sarmiento en la barranca sur del Lago Colhue Huapi, provincia del Chubut: Revista de la Asociación Geológica Argentina, v. XXXIV, p. 271–281.

Strömberg, C.A.E., 2003, The origin and spread of grass-dominated ecosystems during the Tertiary of North America and how it relates to the evolution of hypsodonty in equids: University of California Berkeley.

Strömberg, C.A.E., 2009, Methodological concerns for analysis of phytolith assemblages: Does count size matter?: Quaternary International, v. 193, p. 124–140, https://doi.org/10.1016/j.quaint.2007.11.008.

Strömberg, C.A.E., 2011, Evolution of grasses and grassland ecosystems: Annual Review of Earth and Planetary Sciences, v. 39, p. 517–544, https://doi.org/10.1146/annurev-earth-040809-152402.

Strömberg, C.A.E., Dunn, R.E., Madden, R.H., Kohn, M.J., and Carlini, A.A., 2013, Decoupling the spread of grasslands from the evolution of grazer-type herbivores in South America: Nature Communications, v. 4, 1478, https://doi.org/10.1038/ncomms2508.

Strömberg, C.A.E., Dunn, R.E., Crifò, C., and Harris, E.B., 2018, Phytoliths in Paleoecology, *in* Croft, D.A., Su, D.F., and Simpson, S.W., eds., Methods in Paleoecology—Reconstructing Cenozoic Terrestrial Environments and Ecological Communities: Cham, Switzerland, Springer International Publishing, Vertebrate Paleobiology and Paleoanthropology Series, p. 235–287, https://doi.org/10.1007/978-3-319-94265-0.

Strömberg, C.A.E., Saylor, B.Z., Engelman, R.K., Catena, A.M., Hembree, D.I., Anaya, F., and Croft, D.A., 2024, The flora, fauna, and paleoenvironment of the late Middle Miocene Quebrada Honda Basin, Bolivia (Eastern Cordillera, Central Andes): Palaeogeography, Palaeoclimatology, Palaeoecology, v. 656, https://doi.org/10.1016/j.palaeo.2024.112518.

Sundell, K.E., Gehrels, G.E., and Pecha, M.E., 2021, Rapid U-Pb geochronology by laser ablation multi-collector ICP-MS: Geostandards and Geoanalytical Research, v. 45, p. 37–57, https://doi.org/10.1111/ggr.12355.

Sylwan, C.A., 2001, Geology of the Golfo San Jorge Basin, Argentina: Journal of Iberian Geology, v. 27, p. 123–157.

Trayler, R.B., Schmitz, M.D., Cuitiño, J.I., Kohn, M.J., Bargo, M.S., Kay, R.F., Strömberg, C.A.E., and Vizcaíno, S.F., 2020, An improved approach to age-modeling in deep time: Implications for the Santa Cruz Formation, Argentina: Geological Society of America Bulletin, v. 132, p. 233–244, https://doi.org/10.1130/B35203.1.

Utescher, T., and Mosbrugger, V., 2007, Eocene vegetation patterns reconstructed from plant diversity—A global perspective: Palaeogeography, Palaeoclimatology, Palaeoecology, v. 247, p. 243–271, https://doi.org/10.1016/j.palaeo.2006.10.022.

Vermeesch, P., 2018, IsoplotR: A free and open toolbox for geochronology: Geoscience Frontiers, v. 9, p. 1479–1493, https://doi.org/10.1016/j.gsf.2018.04.001.

Vulinec, K., 2002, Dung beetle communities and seed dispersal in primary forest and disturbed land in Amazonia 1: Biotropica, v. 34, p. 297–309, https://doi.org/10.1111/j.1744-7429.2002.tb00541.x.

Wang, J.W., Gehrels, G., Kapp, P., and Sundell, K., 2023, Evidence for regionally continuous Early Cretaceous sinistral shear zones along the western flank of the Coast Mountains, coastal British Columbia, Canada: Geosphere, v. 19, p. 139–162, https://doi.org/10.1130/GES02502.1.

Westerhold, T., et al., 2020, An astronomically dated record of Earth's climate and its predictability over the last 66 million years: Science, v. 369, p. 1383–1387, https://doi.org/10.1126/science.aba6853.

Wilf, P., Johnson, K.R., Cúneo, N.R., Smith, M.E., Singer, B.S., and Gandolfo, M.A., 2005, Eocene plant diversity at Laguna del Hunco and Río Pichileufú, Patagonia, Argentina: American Naturalist, v. 165, p. 634–650, https://doi.org/10.1086/430055.

Wilf, P., Cuneo, N.R., Escapa, I.H., Pol, D., and Woodburne, M.O., 2013, Splendid and seldom isolated: The paleobiogeography of Patagonia: Annual Review of Earth and Planetary Sciences, v. 41, p. 561–603, https://doi.org/10.1146/annurev-earth-050212-124217.

Wing, S.L., and Greenwood, D.R., 1993, Fossils and fossil climate: The case for equable continental interiors in the Eocene: Philosophical Transactions of the Royal Society of London, Series B: Biological Sciences, v. 341, p. 243–252, https://doi.org/10.1098/rstb.1993.0109.

Wolfe, J.A., 1985, Distribution of major vegetational types during the Tertiary, *in* Sundquist, E.T., and Broecker, W.S., eds., The Carbon Cycle and Atmospheric CO_2: Natural Variations Archean to Present: American Geophysical Union Geophysical Monograph, v. 32, p. 357–375, https://doi.org/10.1029/GM032p0357.

Woodburne, M.O., Goin, F.J., Bond, M., Carlini, A.A., Gelfo, J.N., López, G.M., Iglesias, A., and Zimicz, A., 2014, Paleogene land mammal faunas of South America; a response to global climatic changes and indigenous floral diversity: Journal of Mammalian Evolution, v. 21, p. 1–73, https://doi.org/10.1007/s10914-012-9222-1.

Wotzlaw, J.-F., Schaltegger, U., Frick, D.A., Dungan, M.A., Gerdes, A., and Günther, D., 2013, Tracking the evolution of large-volume silicic magma reservoirs from assembly to supereruption: Geology, v. 41, p. 867–870, https://doi.org/10.1130/G34366.1.

Zachos, J., Pagani, M., Sloan, L., Thomas, E., and Billups, K., 2001, Trends, rhythms, and aberrations in global climate 65 Ma to Present: Science, v. 292, p. 686–693, https://doi.org/10.1126/science.1059412.

Zanazzi, A., Kohn, M.J., MacFadden, B.J., and Terry, D.O., 2007, Large temperature drop across the Eocene–Oligocene transition in central North America: Nature, v. 445, p. 639–642, https://doi.org/10.1038/nature05551.

Ziegler, A.M., Eshel, G., Rees, P.M., Rothfus, T.A., Rowley, D.B., and Sunderlin, D., 2003, Tracing the tropics across land and sea: Permian to present: Lethaia, v. 36, p. 227–254, https://doi.org/10.1080/00241160310004657.

Zucol, A.F., Brea, M., and Bellosi, E.S., 2010, Phytolith studies in Gran Barranca (central Patagonia, Argentina): The middle-late Eocene, *in* Madden, R.H., Carlini, A.A., Vucetich, M.G., and Kay, R.F., eds., The Paleontology of Gran Barranca: Evolution and Environmental Change through the Middle Cenozoic of Patagonia, Cambridge, UK, Cambridge University Press, p. 317–340.

Zucol, A.F., Krause, J.M., Brea, M., Raigemborn, M.S., and Matheos, S.D., 2018, Emergence of grassy habitats during the greenhouse-icehouse systems transition in the middle Eocene of southern South America: Ameghiniana, v. 55, p. 451–482, https://doi.org/10.5710/AMGH.12.03.2018.3152.